nature human behaviour

ARTICLES

DOI: 10.1038/s41562-017-0225-z

Differential hemispheric and visual stream contributions to ensemble coding of crowd emotion

Hee Yeon Im[1,2], Daniel N. Albohn[3], Troy G. Steiner[3], Cody A. Cushing[2], Reginald B. Adams, Jr[3] and Kestutis Kveraga[1,2*]

In crowds, where scrutinizing individual facial expressions is inefficient, humans can make snap judgments about the prevailing mood by reading 'crowd emotion'. We investigated how the brain accomplishes this feat in a set of behavioural and functional magnetic resonance imaging studies. Participants were asked to either avoid or approach one of two crowds of faces presented in the left and right visual hemifields. Perception of crowd emotion was improved when crowd stimuli contained goal-congruent cues and was highly lateralized to the right hemisphere. The dorsal visual stream was preferentially activated in crowd emotion processing, with activity in the intraparietal sulcus and superior frontal gyrus predicting perceptual accuracy for crowd emotion perception, whereas activity in the fusiform cortex in the ventral stream predicted better perception of individual facial expressions. Our findings thus reveal significant behavioural differences and differential involvement of the hemispheres and the major visual streams in reading crowd versus individual face expressions.

We routinely encounter groups of people at work, school or social gatherings. In real-life situations, we often need to make quick decisions about which group of people to approach or avoid, and the facial expressions of the group members play an important role in our judgments of their intent and predisposition. As such decisions usually need to be made rapidly in many social situations, serial scrutiny of each individual's facial expression is slow and becomes increasingly inefficient as the size of the crowd grows. Instead, extracting summary statistics (that is, the average) through a process known as ensemble coding[1–4] is a more efficient way to process an array of similar objects.

A large body of evidence has shown that the visual system can rapidly extract the average of multiple stimulus features such as the orientation[5,6], size[7,8] and motion direction[9] of groups of objects in an array. Ensemble coding provides precise global representation[1,7,8,10] with little or no conscious perception[6,7,11–13] or sampling of individual members in a set[14,15]. Recent work has further shown that ensemble coding occurs for even more complex objects, such as averaging emotion from sets of faces[2,3,16–19] and facial identity[16,20–23], as well as a crowd's movements[24,25] and gaze direction[26,27].

Face perception has great social importance because emotional expressions forecast the behavioural intentions of the expressors[28–30] and govern observers' fundamental social motivations accordingly. From a perceiver's perspective, for example, an angry face elicits an avoidance reaction while a happy face elicits an approach reaction[28,30–32]. To date, however, empirical work undertaken on ensemble perception of faces has largely concentrated on the efficiency and the fidelity of crowd perception[2,3,16–23], but not on how this process is socially relevant. To our knowledge, no studies have examined how humans make speeded social decisions about which crowd of faces to approach or avoid, based on extracted ensemble features of facial crowds (for example, crowd emotion). We often engage in such affective appraisals to enhance our social life (for example, looking for a more approachable group of people to have a chat with at a cocktail party) and, occasionally, to avoid danger (for example, rapidly inferring intent to commit violence from the facial expressions of a mob on the street to enable oneself to escape in time and seek help from another group that looks kinder).

Therefore, in the current study we aimed to characterize the behavioural and neural mechanisms of social decision-making based on rapidly extracted crowd emotion from groups of faces. Behaviourally, our goals were to examine (1) how extracting crowd emotion from two groups of faces was modulated by task demands reflecting different social motivations (approach or avoidance) and whether this processing was significantly lateralized across the visual field and (2) how the characteristics of facial crowds such as sex-linked identity cues and group size interact with the social motivations present when perceiving crowd emotion. These factors have received surprisingly little attention in the literature of ensemble perception of facial crowds, although they have been found to play a major role in affective processing elsewhere[28–30,33–39].

Neurally, our goal was to examine the brain networks and pathways mediating ensemble perception of crowd emotion and compare them to the neural processes underlying the extraction of emotion from, and choice between, two individual faces. We focused on the dorsal and ventral visual streams, predicting their preferential involvement in processing crowd and individual emotion, respectively. The magnocellular (M) and parvocellular (P) pathways project primarily, but not exclusively, to the dorsal and ventral streams, respectively[40,41]. The dorsal M-dominant pathway is suggested to support vision for action, non-conscious vision and detection of global and low-frequency information, whereas the ventral P-dominant pathway is suggested to support vision for perception, conscious vision and analysis of local, high spatial frequency information[42–52]. Given such distinctive properties and functions of the dorsal and ventral pathways, we hypothesized that

[1]Department of Radiology, Harvard Medical School, Charlestown, MA 02129, USA. [2]Athinoula A. Martinos Center for Biomedical Imaging, Department Radiology, Massachusetts General Hospital, Charlestown, MA 02129, USA. [3]Department of Psychology, The Pennsylvania State University, State College, PA, 16802 USA. *e-mail: kestas@nmr.mgh.harvard.edu

© 2017 Macmillan Publishers Limited, part of Springer Nature. All rights reserved.

decisions on rapidly extracted global information of crowd emotion may rely on dorsal pathway-dominant processing, whereas decisions that involve comparison between two individual emotional faces may rely on ventral pathway-dominant processing. We tested this hypothesis using both whole-brain and region of interest (ROI) analyses in the superior frontal gyrus (SFG) and the intraparietal sulcus (IPS), which have been implicated as conveying information via the M-pathway[53–57], and the fusiform gyrus (FG), which is known to support P-pathway information[38,56,58–62]. Finally, we also included the amygdala as an additional ROI, given its central role in emotional processing[63–68]. Unlike the other ROIs (the IPS, SFG and FG), which we predicted to be selectively engaged in reading crowd versus individual emotion, we expected that the amygdala would be involved in both processes.

To accomplish our goals, we conducted a set of behavioural and functional magnetic resonance imaging (fMRI) experiments in which participants viewed visual stimuli containing two groups of faces with varying emotional expressions (single faces were also examined for a direct comparison in the fMRI study), presented in the left and right visual hemifields. Participants were asked to choose one of the two crowds (or individual faces) as rapidly as possible, to indicate which they would avoid or approach. Unlike the estimation task in which the absolute value is judged, the answers and the ease of the decision in such a comparison task varied depending on the task goal. For example, the decision to choose to approach a happy crowd versus an emotionally neutral crowd should be quite clear and explicit. However, the same comparison (happy versus neutral) becomes more ambiguous and implicit when observers have to decide which crowd they would rather avoid. This paradigm allows us to examine the role of observers' social motivation in comparing crowd emotion and its interaction with crowd size, sex-linked identity cues and visual field of presentation.

Results

Experiment 1: behavioural study. Participants viewed two crowds of faces (Fig. 1b)—one in the left visual field (LVF) and one in the right visual field (RVF)—for 1 s. They were instructed to fixate on the centre fixation cross and to make a key press as quickly and accurately as possible to indicate which group of faces they would rather avoid (experiment 1a) or approach (experiment 1b). Rather than freely choosing, participants were explicitly informed that the correct answer was to choose the crowd that looked angrier in the avoidance task and the crowd that looked happier on average in the approach task. This allowed us to create task settings that were applicable in the naturalistic social context, by instructing participants to make relative comparisons between two crowds or faces in order to achieve the explicit social goal (for example, avoiding a more threatening crowd or approaching a friendlier crowd).

The individual faces contained in each crowd were chosen from a set of 51 faces (Fig. 1a) morphed from two highly intense, prototypical facial expressions (angry and happy) of the same person. The set contained six different identities (three male and three female faces) taken from the Ekman face set[69]. One visual field always contained a crowd with varied expressions that were nonetheless emotionally neutral on average (that is, the particular mix of happier and angrier expressions was at the midpoint between happy and angry). The other visual field contained a crowd that had a mix of expressions that was either happier or angrier on average than the neutral crowd. Individual faces all had different emotional intensities, and half of the individual faces were more intense in the neutral crowd than any expression in the emotional crowd. This is critical because it ensures that participants could not simply rely on finding the most intense (happy or angry) expression and base their decision on that face. Instead, they had to choose the crowd to approach or avoid based on the average emotion from a crowd in order to perform the task correctly.

While participants reported the task as being rather difficult, they could reliably perform the task at levels well above chance. The overall accuracies for both experiments 1a and 1b were significantly higher than chance (avoidance task: 64.88 versus 50%; approach task: 63.72 versus 50%; all P values < 0.001 from separate one-sample t-tests), demonstrating that participants were able to extract the average crowd emotion from the two groups of faces and choose appropriately which group they would rather avoid or approach. Although accuracies for the avoidance task versus approach task were not significantly different (64.88 versus 63.72%, $t_{40} = 1.330$, $P = 0.191$), the mean response time (RT) was significantly slower for the avoidance task than the approach task (1.17 versus 0.98 s, $t_{40} = 2.156$, $P < 0.04$, Cohen's $d = 0.666$). We also conducted RT analyses using each participant's median RT. As for the mean RT, the median RT was significantly slower for the avoidance task than the approach task (1.16 versus 0.97 s on average: $t_{40} = 1.995$, $P < 0.05$, Cohen's $d = 0.632$). We also confirmed that median RTs yielded the same results for all the other findings reported in this paper (see Supplementary Results). As shown in Fig. 1d, neither accuracy nor RT was affected by the size of the facial crowd (8 versus 12 faces in total) in either the avoidance task (accuracy: $t_{40} = 0.113$, $P > 0.250$, Cohen's $d = 0.035$; RT: $t_{40} = 0.010$, $P > 0.250$, Cohen's $d = 0.003$) or approach task (accuracy: $t_{40} = 0.818$, $P > 0.250$, Cohen's $d = 0.153$; RT: $t_{40} = -0.037$, $P > 0.250$, Cohen's $d = -0.011$), suggesting that extraction of crowd emotion does not require serial processing of each individual crowd member, but is processed in parallel. As there was no effect of crowd size, we collapsed the data from the different crowd size conditions for further analyses.

Facilitation of task-congruent cues. In our morphing methods (Fig. 1a), the emotional distance between the morphed faces could be quantified based on the arbitrary values of the emotional unit number, with 0 being emotionally ambiguous (for example, 50% happy and 50% angry), +25 being extremely happy (100% happy) and −25 being extremely angry (100% angry). As the neutral crowd (emotional unit of 0 on average) was always presented on one side, a positive value of emotional distance between the two crowds indicated that the other side to be compared contained a happier crowd than the neutral crowd (for example, +9 versus 0 = very happy versus neutral, whereas +5 versus 0 = somewhat happy versus neutral) and a negative value of emotional distance indicated that the other side contained an angrier crowd than the neutral crowd (for example, −9 versus 0 = very angry versus neutral, whereas −5 versus 0 = somewhat angry versus neutral). Such separation proved to be effective in systematically manipulating the difficulty of the task (Fig. 1e). A repeated-measures analysis of variance (ANOVA) showed a significant main effect of the emotional distance (four levels: −9, −5, +5 and +9) on performance accuracy in both the avoidance task ($F_{3,60} = 4.69$, $P < 0.01$, partial eta squared, $\eta_p^2 = 0.29$) and the approach task ($F_{3,60} = 4.644$, $P < 0.01$, $\eta_p^2 = 0.219$). Post hoc Tukey's honest significant difference (HSD) pairwise comparison tests revealed higher accuracy for an emotional distance of +9 than +5, as well as higher accuracy for an emotional distance of −9 than −5 (all P values < 0.05), suggesting that accuracy increased when the emotional distance between the two crowds being compared increased in both the avoidance and approach tasks.

Furthermore, contrast analyses also revealed that participants were more accurate for the crowd emotion that was congruent with the task goal—whether to approach or avoid. That is, participants were more accurate when comparing angry versus neutral crowds (both levels of emotional distance: −9 and −5) than happy versus neutral crowds (both levels of emotional distance: +9 and +5) during the avoidance task, which was statistically confirmed by the contrast of −9 and −5 versus +9 and +5 ($t_{80} = 2.37$, $P < 0.03$). Conversely, during the approach task, participants were more accu-

© 2017 Macmillan Publishers Limited, part of Springer Nature. All rights reserved.

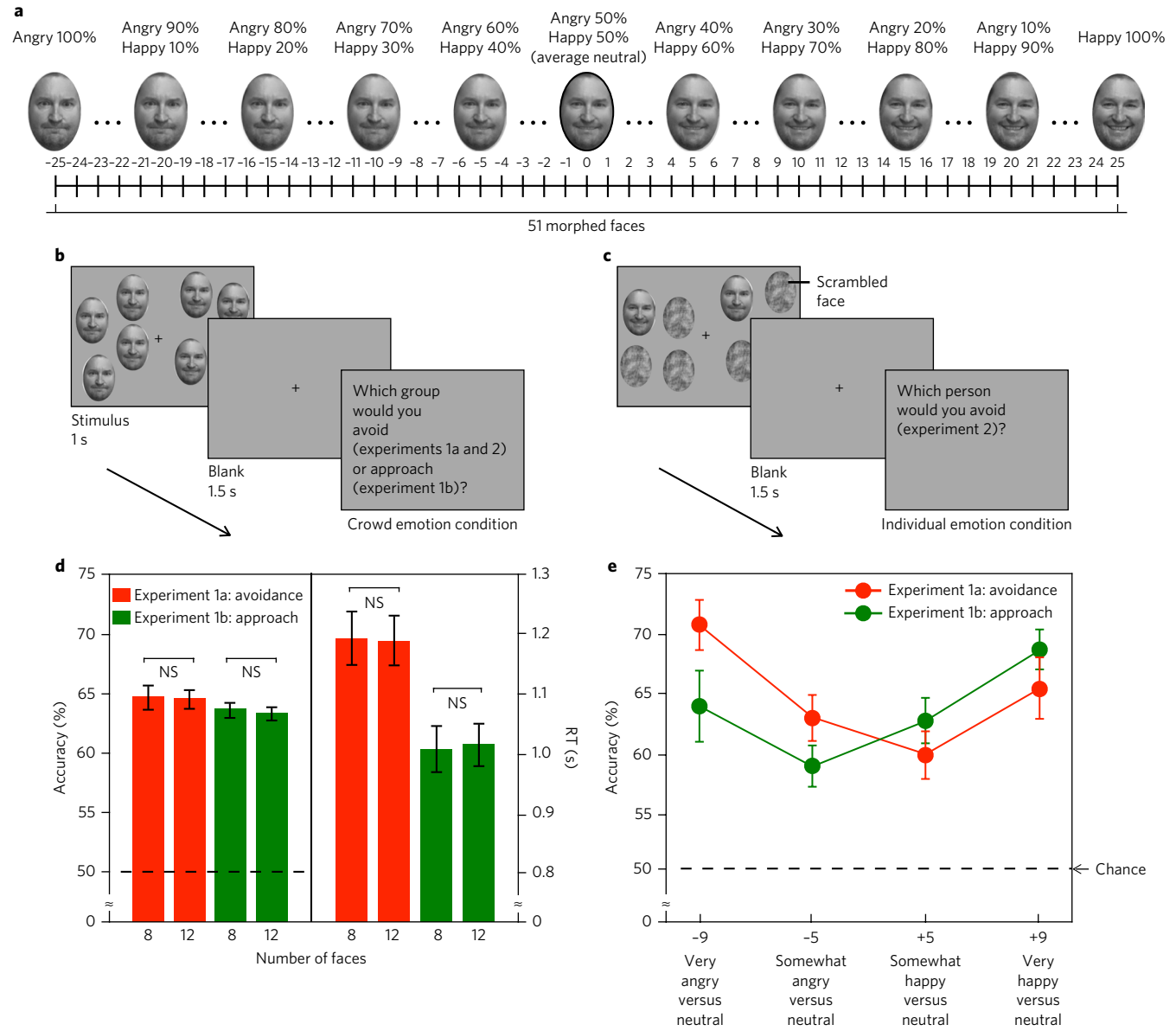

Fig. 1 | Sample face images, sample trials of crowd emotion and individual emotion conditions, and the results from experiment 1. a, Examples of 51 morphed faces from two extremely angry and happy faces of the same person, with −25 emotional units being extremely angry, 0 being neutral, and +25 being extremely happy. Ekman face images used in the actual experiments are replaced in these figures due to copyright. **b**, Sample trial of crowd emotion condition. **c**, Sample trial of the individual emotion condition (included in the fMRI study). **d**, Effect of the number of faces on the accuracy and RT in experiment 1a (avoidance task, red bars) and experiment 1b (approach task, green bars). The error bars indicate the standard error of the mean (s.e.m.). NS, not significant. **e**, Effect of the similarity in average emotion between facial crowds on crowd emotion processing: participants' accuracies in experiment 1a (avoidance task, red line) and experiment 1b (approach task, green line) are plotted as a function of the emotional distance in emotional units between two facial crowds to be compared. The error bars indicate the standard error of the mean (s.e.m.).

rate when comparing happy versus neutral crowds (both levels of emotional distance: +9 and +5) than angry versus neutral crowds (both levels of emotional distance: −9 and −5) ($t_{80}=2.12$, $P<0.04$). The RTs showed similar trends towards faster RTs for comparisons involving task-congruent crowd emotion: angry versus neutral (emotional distance of −9 and −5) for the avoidance task and happy versus neutral (emotional distance of +9 and +5) for the approach task (Supplementary Result 1). Together, these results suggest that observers were most accurate and efficient when they had to choose angrier crowds over neutral for the avoidance task and happier crowds over neutral for the approach task. Thus, it appears that motivational information systematically modulates observers' evaluation of crowd emotion.

Right hemisphere dominance for goal-relevant crowd emotion. When participants judged which crowd they would avoid (experiment 1a), choosing an angry crowd over a neutral crowd was an easier, task-congruent decision (red frame shown in Fig. 2a). In contrast, choosing a neutral over a happy crowd introduces ambiguity into the decision, because the neutral crowd does not contain an explicit social cue (although it is less friendly than a happy crowd, it is not angry on average; grey frame shown in Fig. 2a). In both types of decisions, we observed right hemisphere (RH) dominance in which participants' accuracy was facilitated when the facial crowd to be chosen was presented in the LVF. Their accuracy was higher for an angry crowd presented in the LVF than the RVF when comparing an angry versus a neutral crowd. Accuracy was also higher for a

© 2017 Macmillan Publishers Limited, part of Springer Nature. All rights reserved.

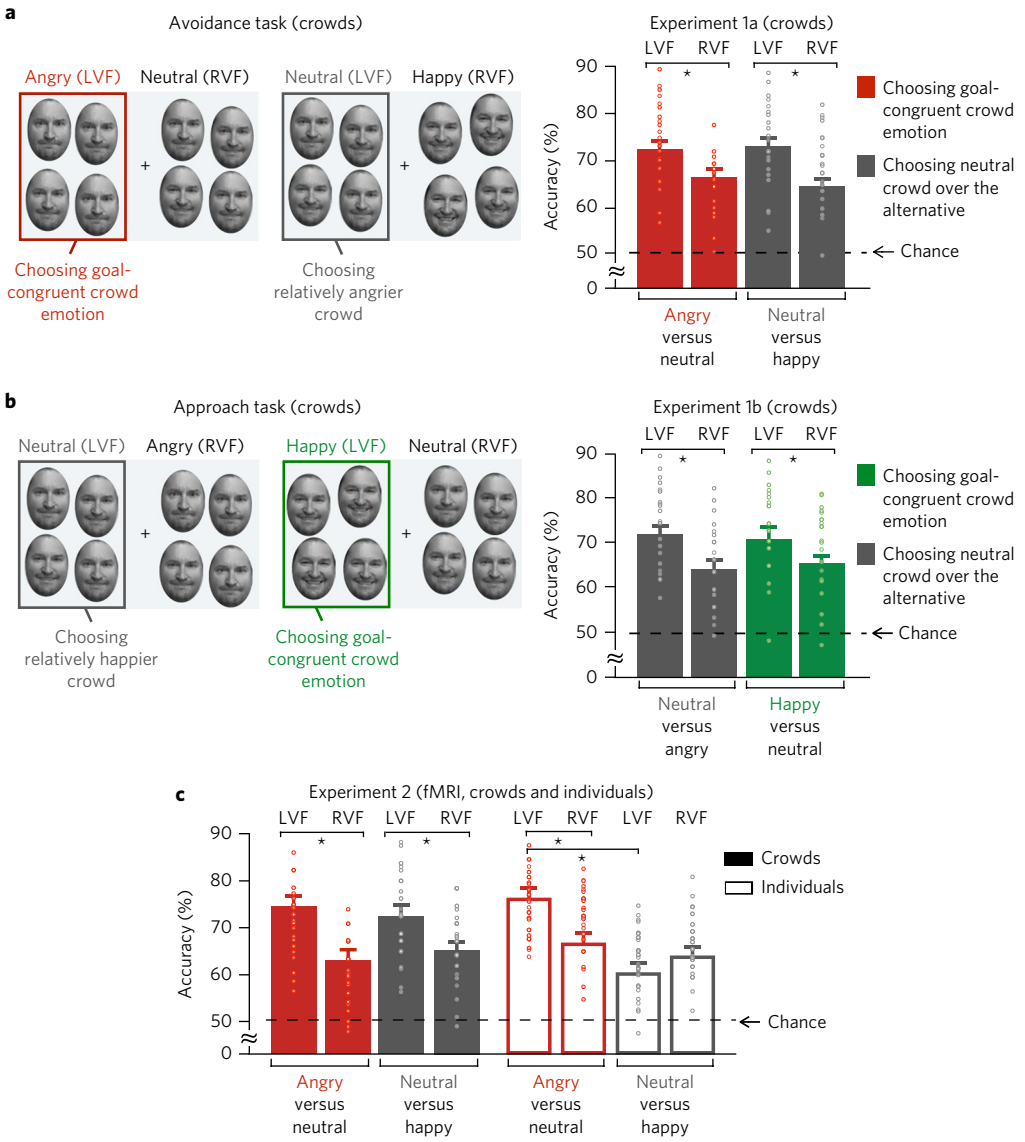

Fig. 2 | RH dominance for goal-relevant crowd emotion in crowd emotion processing. a, Participants' accuracy for the avoidance task (experiment 1a), separately plotted for when the crowd to be chosen (an angry crowd compared with a neutral crowd or a neutral crowd compared with a happy crowd) is presented in the LVF versus the RVF. As the correct answer was to choose the 'relatively angrier' crowd, participants had to choose an angry over a neutral crowd and a neutral over a happy crowd. Ekman face images used in the actual experiments are replaced in these figures due to copyright. **b**, Participants' accuracy for the approach task (experiment 1b), separately plotted for when the crowd to be chosen (a happy crowd compared with a neutral crowd or a neutral crowd compared with an angry crowd) is presented in the LVF versus the RVF. Note that the valence of the goal-relevant crowd emotion is switched from angry to happy in the approach task. **c**, Participants' accuracy in experiment 2 (the fMRI study). Accuracies for both the crowd emotion and individual emotion conditions are plotted for the LVF and RVF separately. The points in **a**–**c** represent data from individual participants, the error bars indicate the s.e.m. and the asterisks indicate statistically significant differences at $P < 0.05$.

neutral crowd presented in the LVF than the RVF when comparing a neutral versus a happy crowd during the avoidance task (Fig. 2a). A two-way repeated measures ANOVA with two factors—the visual field of presentation (LVF versus RVF) and the emotional valence of the crowd to be chosen (angry versus neutral)—revealed a significant main effect of the visual field ($F_{1,20} = 6.133$, $P < 0.03$, $\eta_p^2 = 0.235$), with accuracy for LVF presentation being greater than for RVF presentation. The main effects of the emotional valence of the crowd to be chosen ($F_{1,20} = 0.033$, $P = 0.858$, $\eta_p^2 = 0.002$) and the interaction ($F_{1,20} = 0.818$, $P = 0.376$, $\eta_p^2 = 0.039$) were not significant. Post hoc Tukey's HSD pairwise comparison tests confirmed both the higher accuracy for an angry crowd in the LVF than an angry crowd in the RVF ($P < 0.05$) and the higher accuracy for a neutral crowd in the LVF than a neutral crowd in the RVF ($P < 0.04$). This result indicates hemispheric specialization for crowd emotion processing in which LVF/RH presentations are superior for crowd emotion to be chosen (an angry over a neutral crowd and a neutral over a happy crowd) for the avoidance task.

In contrast, for the approach task (experiment 1b), participants had to choose which of the two crowds they would rather approach. It is important to note that the emotional valence of the congruent social cue for the approach task is opposite to that for the avoidance task. For the approach task, choosing a happy over a neutral crowd is a task-congruent social decision (Fig. 2b), whereas choosing a neutral over an angry crowd is a more ambiguous decision (grey frame shown in Fig. 2b). Despite the emotional valence of a

© 2017 Macmillan Publishers Limited, part of Springer Nature. All rights reserved.

task-congruent social cue being flipped (for example, angry for an avoidance task and happy for an approach task), we again found a consistent pattern of hemispheric asymmetry. The participants' accuracy for crowd emotion to be chosen (a happy crowd when comparing a happy versus a neutral crowd and a neutral crowd when comparing a neutral versus an angry crowd) was facilitated when it was presented in the LVF compared with the RVF (Fig. 2b). A two-way repeated measures ANOVA showed the significant main effect of the visual field ($F_{1,20}=5.447$, $P<0.05$, $\eta_p^2=0.232$), although the main effect of the emotional valence of the crowd to be chosen (happy versus neutral: $F_{1,20}=0.358$, $P=0.556$, $\eta_p^2=0.019$) and the interaction ($F_{1,20}=0.654$, $P=0.428$, $\eta_p^2=0.035$) were not significant. Post hoc Tukey's HSD pairwise comparison tests also confirmed the higher accuracy both for a happy crowd in the LVF compared with the RVF ($P<0.04$) and a neutral crowd in the LVF compared with the RVF ($P<0.02$). The RT results also indicated faster processing of crowds containing task-congruent cues than crowds containing task-incongruent cues, both for the avoidance and approach tasks (more details and statistics are reported in Supplementary Result 1).

Because of the relative comparisons required in our study, in the avoidance task, a neutral crowd could be either the one to be avoided when compared with a happy crowd or the one not to be avoided when compared with an angry crowd. Similarly, in the approach task, a neutral crowd could be either the one to be approached when compared with an angry crowd or the one not to be approached when compared with a happy crowd. One could imagine that on a given trial a neutral crowd was the avoidance/approach stimulus but on the next trial it was the non-avoided/non-approached stimulus, depending on the other crowd. If participants had used different cognitive strategies for the comparisons of an angry versus a neutral crowd and a happy versus a neutral crowd within the same task, switching the response mapped to a neutral crowd from one trial to the next could significantly slow down participants' RT or impair their accuracy because of the switch cost[70–74]. To examine whether such previous trial interference occurred, we compared participants' RT and accuracy when the response mapped onto a neutral crowd was switched (switched trials) versus when the same type of comparison was repeated (repeated trials). We found no difference in the RT or accuracy between switch trials versus repeated trials in the avoidance task or the approach task (all P values >0.570; more details shown in Supplementary Result 9), suggesting that the previous trial interference effects and switching costs were minimal in our task.

Together, our results are consistent with previous studies that have shown that the RH is dominant for global processing whereas the left hemisphere (LH) is dominant for local processing[75–79]. Furthermore, our results suggest that the RH dominance for global processing of crowd emotion is also modulated by the task goal at hand. Regardless of the actual emotional valence of the facial crowd, LVF/RH processing facilitated processing of a goal-relevant facial crowd: processing of a facial crowd that looked 'relatively angrier' was facilitated during the avoidance task, whereas processing of a facial crowd that looked 'relatively happier' was facilitated during the approach task.

Sex-specific identity cues that modulate crowd emotion perception. Because previous findings of individual face perception have documented that female- and male-specific facial features are perceptually confounded with happy and angry expressions, respectively[33,80], we examined whether processing of crowd emotion was also modulated by sex-specific facial identity cues. We compared the accuracy for male and female facial crowd stimuli (illustrated in Fig. 3a) in the avoidance and approach tasks. Figure 3b,c shows the accuracy on the avoidance task and approach task, plotted separately by the valence of emotional face images (happy and angry) to be compared with a neutral crowd and the sex of the face images (male versus female). The two-way repeated-measures ANOVA showed that the main effects of stimulus sex ($F_{1,20}=2.984$, $P=0.100$) and emotional valence of the face images ($F_{1,20}=0.112$, $P=0.741$) were not significant in the avoidance task. In the approach task, the main effect of stimulus sex ($F_{1,20}=4.966$, $P<0.04$, $\eta_p^2=0.199$) was significant, but the main effect of emotional valence ($F_{1,20}=0.588$, $P=0.981$) was not, with the accuracy for female crowds being greater. Importantly, we found a significant interaction between the sex and the emotion of the facial crowd both in the avoidance task ($F_{1,20}=4.908$, $P<0.04$, $\eta_p^2=0.197$) and the approach task ($F_{1,20}=4.678$, $P<0.05$, $\eta_p^2=0.190$). Post hoc Tukey's HSD pairwise comparison tests showed a higher accuracy for angry male than angry female crowds ($P<0.05$) in the avoidance task and a higher accuracy for happy female than happy male crowds in the approach task ($P<0.04$). These results suggest that integration of crowd emotion from emotional faces is also influenced by sex-specific identity cues.

Comparing the differing task demands for avoidance and approach, we also observed a modulation by task demands. Contrast analyses comparing the accuracy for angry males with the other three conditions (happy males, angry females and happy females) revealed that participants were most accurate when comparing an angry male crowd versus a neutral male crowd than the other three conditions during the avoidance task ($t_{80}=2.119$, $P<0.05$), suggesting that facial anger and masculine features both conveyed threat cues and interacted to facilitate decisions to avoid a crowd. Conversely, participants were most accurate in comparing a happy female crowd versus a neutral female crowd than the other three conditions during the approach task ($t_{80}=2.473$, $P<0.02$). Although the sex of the faces in our crowd stimuli modulated the perception of crowd emotion, we found that the sex of the participants did not influence perception of crowd emotion either in the avoidance or the approach task (Supplementary Result 2).

Reading crowd emotion from faces of different identities. In real-world situations, compared with a laboratory, we never view one person's various emotional expressions simultaneously. Rather, we encounter groups of individuals who differ not only in their emotional expression, but also identity, age and gender cues. As a majority of the previous studies of average crowd emotion (including the main experiments in the current study, but see ref. [19]) constructed each stimulus using faces of the same person that varied in emotionality, observers' ability to extract crowd emotion from facial expressions of the same individual versus from different individuals has not yet been directly compared. Thus, we conducted two control experiments (1a and 1b) in which two new groups of participants ($n=40$ in total) were presented with crowd stimuli containing a mix of different identities (Supplementary Result 3). As in our main experiments, the task was to choose the relatively angrier crowd of the two to avoid (avoidance task; control experiment 1a) and to choose the relatively happier crowd to approach (approach task; control experiment 1b). As we report in detail in Supplementary Result 3, we replicated the results of main experiments 1a and 1b even with mixed presentation of different facial identities and with new cohorts of participants. We obtained not only similar overall accuracy and overall RT results, but also the replication of the task-goal-dependent facilitation of the accuracy and the RH dominance for crowd emotion to be chosen. These results suggest that facial identity cues do not significantly interfere with extraction of crowd emotion. They also confirm the robustness of our main findings of task-goal-dependent modulation and hemispheric asymmetry for task-congruent and task-incongruent decisions on crowd emotion.

Parallel, global processing of facial crowds (eye tracking study). In both experiments 1a (avoidance) and 1b (approach), we found that

© 2017 Macmillan Publishers Limited, part of Springer Nature. All rights reserved.

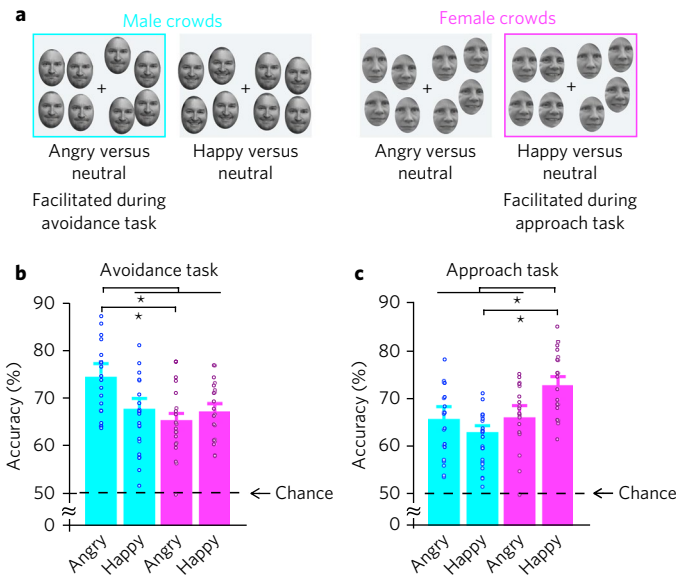

Fig. 3 | Effect of the sex-specific identity cue of facial crowds on crowd emotion perception. a, Sample crowd stimuli for male (cyan) and female (magenta) crowds. Ekman face images used in the actual experiments are replaced in these figures due to copyright. **b**, Participants' accuracy in the avoidance task (experiment 1a) depending on the sex of the facial crowds (male crowds versus female crowds) and the emotional valence of the emotional crowd (angry versus happy). **c**, Participants' accuracy for the approach task (experiment 1b). The points in **b** and **c** represent data from individual participants, the error bars indicate the s.e.m. and the asterisks indicate statistically significant differences at $P < 0.05$.

presenting a larger number of faces in facial crowds (from 8 to 12 in total) did not impair participants' accuracy or slow down their RT (Fig. 1d). Likewise, in control experiments 1a and 1b (Supplementary Result 3), we observed no set size effects on the accuracy or RT, suggesting that participants did not process each individual crowd member in a serial manner (see also Supplementary Result 8 for further analyses and discussion). However, it is still possible that a total duration of 2.5 s for the stimulus (1 s) and blank (1.5 s) presentation was sufficient for participants to saccade rapidly to only two or three faces in each visual field to make a judgment relying only on these sampled subsets. If this were the case, the flat slope between 8 and 12 faces both in the accuracy and the RT could also be observed as a result of serial processing of subsets, rather than parallel processing. To address this issue, we conducted control experiment 2 in which a new group of 18 participants performed the same avoidance task as in experiment 1a, with their eye movement monitored and restricted (fixed to the centre of the screen) throughout the experiment. We observed not only that both the accuracy and RT were comparable to our main results from experiment 1a (and control experiment 1a), but also that the effects of the set size, the emotional distance and the goal-dependent hemispheric lateralization were replicated in this control eye-tracking experiment. All the details and statistics of control experiment 2 are reported in Supplementary Result 4. These results provide evidence that extracting crowd emotion of facial groups does not necessarily require participants to make eye saccades towards a subset of individual faces. Therefore, we conclude that crowd emotion can be extracted as a whole, in a parallel manner rather than relying on serial processing of individual faces or subjects of faces in crowds.

Experiment 2: fMRI study. For the fMRI study, we scanned 30 participants, using only the avoidance task because of time and budgetary constraints. Participants were presented with stimuli containing either two facial crowds (Fig. 1b) or two single faces presented in a crowd of scrambled masks (Fig. 1c). Participants were asked to choose rapidly which of the two facial crowds (crowd emotion condition) or which of the two single faces (individual emotion condition) they would rather avoid, using an event-related design with crowd emotion and individual faces conditions randomly intermixed (see Methods for more details). We compared the patterns of brain activation when participants chose to avoid one of two crowds or one of two individual faces. If the processing of crowd emotion relies on the same mechanism that mediates single face perception, we would observe activations of the same brain network during the processing of crowd emotion, but perhaps to a larger extent than during single face comparisons, given the greater complexity of the stimulus and difficulty of the crowd emotion task. Alternatively, if the processing of crowd emotion and individual face emotion relies on qualitatively distinct processes, specifically mediated by dorsal and ventral visual pathways as we hypothesized, we would expect to observe differential brain activations in distinct sets of brain areas in dorsal and ventral visual pathways.

Behavioural results. The participants' overall accuracy for crowd emotion condition in the fMRI study was 63.16%, which was not significantly different from that observed in experiment 1a (64.88%; $t_{48} = -1.468$, $P = 0.149$). We further confirmed that the behavioural results of the crowd emotion condition in the fMRI study replicated other behavioural results in experiment 1a and the control experiments. Participants' accuracy was higher when the emotional distance between the two crowds being compared increased, when comparing angry (task-congruent cue) versus neutral crowds compared with happy versus neutral crowds and when comparing angry male versus neutral male crowds compared with angry female versus neutral female crowds. The figures and statistical tests supporting these results are presented in Supplementary Result 5.

Critically, we again replicated the RH advantage for crowd emotion to be chosen, as in experiment 1a (Fig. 2a) and the control experiments (Supplementary Results 3 and 4). The participants' accuracy was higher when the crowd emotion to be chosen was presented in the LVF than the RVF, both for comparisons of an angry versus neutral crowd and a neutral versus happy crowd (Fig. 2c, filled bars). This was confirmed by a significant main effect of the visual field of presentation (LVF versus RVF: $F_{1,29} = 4.560$, $P < 0.05$) from a two-way repeated measures ANOVA, with the accuracy for the LVF being greater than the RVF. The main effect of the emotional valence of the crowd to be chosen was not significant (angry versus neutral: $F_{1,29} = 1.141$, $P = 0.294$), although the interaction was significant ($F_{1,29} = 9.361$, $P < 0.01$). Post hoc Tukey's HSD pairwise comparison tests also confirmed higher accuracy for an angry crowd in the LVF than the RVF ($P < 0.03$) and for a neutral crowd in the LVF than the RVF ($P < 0.05$).

For the individual emotion condition, the overall accuracy was 65.92%, which was slightly but not significantly higher than that for crowd emotion condition ($t_{58} = -1.491$, $P = 0.106$). We also observed no difference in the RT for the crowd emotion condition versus the individual emotion condition ($t_{58} = 0.318$, $P = 0.751$). Even though only two faces were presented—and thus there was no need to extract the average crowd emotion—the level of accuracy and the RT for comparing two individual faces was similar to that for comparing two facial crowds. These results confirm that the difference in our fMRI findings comparing crowd emotion versus individual emotion conditions was not due to a difference in task difficulty, but reflects qualitative differences in neural processing patterns and substrates.

Finally, we observed different patterns of hemispheric lateralization for the individual emotion condition (Fig. 2c, unfilled bars). Unlike the crowd emotion condition showing the RH advantage regardless of the emotional valence of the crowd emotion to be

© 2017 Macmillan Publishers Limited, part of Springer Nature. All rights reserved.

chosen, the individual emotion condition showed that participants' accuracy was higher when an angry face was presented in the LVF/RH and when a neutral face was presented in the RVF/LH. In addition, choosing an angry face over a neutral face was more accurate than choosing a neutral face over a happy face overall. A two-way repeated measures ANOVA showed that the main effect of the visual field of presentation was not significant for the individual emotion condition ($F_{1,29}=1.702$, $P=0.202$), although the main effect of the emotional valence of the face to be chosen (angry versus neutral: $F_{1,29}=18.511$, $P<0.01$) and the interaction ($F_{1,28}=8.193$, $P<0.01$) were significant. Post hoc Tukey's HSD pairwise comparison tests also confirmed a higher accuracy for an angry face in the LVF than in the RVF ($P<0.05$) and a higher accuracy for an angry face than a neutral face in the LVF ($P<0.05$), but not in the RVF ($P>0.76$). Our findings in the individual emotion condition are consistent with previous findings suggesting that affective face processing in general is right-lateralized, with more marked laterality effects for negatively valenced stimuli[35,80–82]. Together, our behavioural data from the fMRI study replicate our main findings from experiment 1a (and other control experiments) and provide further evidence that perception of crowd emotion and individual emotion engage different patterns of hemispheric specialization.

fMRI results. *Distinct neural substrates for crowd emotion versus individual emotion processing.* Our main goal in the fMRI experiment was to characterize the neural substrates involved in participants' avoidance decision between two facial crowds versus those mediating decisions between two individual faces. Figure 4a shows the brain regions activated when participants were comparing two crowds (labelled in red) versus two individual faces (labelled in blue). The complete list of activations is reported in Table 1. Using the contrast of crowd emotion condition minus individual emotion condition, we observed that comparing two facial crowds in the avoidance task showed greater cortical activations in the parietal and frontal regions along the dorsal stream (for example, the IPS, superior parietal lobule, SFG, middle frontal gyrus, inferior frontal gyrus and orbitofrontal cortex) in both hemispheres. In contrast, the individual emotion condition evoked greater activation in the regions along the ventral stream (the FG, parahippocampal cortex (PHC), retrosplenial cortex and temporal pole), anterior cingulate cortex (ACC)/posterior cingulate cortex (PCC) and ventromedial prefrontal cortex (PFC). To verify the robustness of our results, we also used several different thresholding parameters ($P<0.001$, uncorrected; extent, $k=5$ in Supplementary Table 1 and $P<0.0005$, uncorrected; $k=5$ in Supplementary Table 2) and observed similar patterns with greater activations in the regions along the dorsal pathway for crowd emotion condition and in the regions along the ventral pathway for individual emotion condition.

We further examined responses in our regions of interest (the IPS, SFG, FG and amygdala). We chose these ROIs based on previous work showing involvement of the SFG in dorsal stream processing and its intrastream functional connectivity with the IPS[53–57], work showing major involvement of the FG in ventral stream information processing[38,56,58–62] and the wealth of data supporting the link between the amygdala and emotional functions in general[63–68]. These regions were functionally restricted based on an unbiased contrast of all the visual conditions minus the baseline (average activation of voxels) using random effects models (height: $P<0.01$, uncorrected; extent: five voxels), within the anatomical label for each ROI (obtained by the anatomical parcellation of the normalized brain[83]). As shown in Fig. 4b, we observed that both the left and right IPS and SFG showed greater activation for the crowd emotion condition than the individual emotion condition, whereas the bilateral FG showed greater activation for the individual emotion condition than the crowd emotion condition (see Supplementary Fig. 10 for a breakdown of the emotional valence for each condition as well). This observation was confirmed by paired *t*-tests (two-tailed), conducted separately for each ROI (crowd emotion > individual emotion: $P<0.01$ for the bilateral IPS and SFG; individual emotion > crowd emotion: $P<0.01$ for the bilateral FG). These results suggest that the regions in the dorsal visual pathway (for example, the IPS and SFG) and ventral visual pathway (for example, the FG) show differential responsivity to crowd emotion and individual emotion comparisons, respectively. Unlike these three ROIs, which showed selective responses to crowd emotion (IPS and SFG) and individual emotion (FG) conditions, we observed that the bilateral amygdala did not distinguish between crowd emotion and individual emotion conditions. The amygdala showed similar levels of responsivity to both conditions, which was confirmed by a non-significant *t*-test for crowd versus individual emotion conditions (two-tailed: $P>0.693$). The null result for amygdala activation suggests that the differential responses of the IPS, SFG and FG observed here are pathway specific.

Furthermore, we found that the activity in these ROIs differentially predicted the participants' behavioural accuracy for the crowd emotion and individual emotion conditions. As shown in Fig. 4c, the responses of the bilateral IPS and the right SFG positively correlated with participants' accuracy for the crowd emotion condition (left IPS: coefficient of correlation (r)$=0.424$, $P<0.01$; right IPS: $r=0.462$, $P<0.01$; left SFG: $r=0.337$, $P=0.069$; right SFG: $r=0.454$, $P<0.02$), whereas the activity of the bilateral FG positively correlated with the accuracy for the individual emotion condition (left FG: $r=0.568$, $P<0.01$; right FG: $r=0.498$, $P<0.01$). However, we did not find any significant correlation between participants' amygdala activity and behavioural accuracy for crowd emotion condition (left amygdala: $r=0.266$, $P=0.155$; right amygdala: $r=0.192$, $P=0.310$) or individual emotion condition (left amygdala: $r=0.133$, $P=0.482$; right amygdala: $r=0.254$, $P=0.176$). Together, our fMRI results provide evidence for differential contributions of the dorsal and ventral visual pathways to crowd emotion and individual emotion processing, respectively.

Finally, we verified that our ROIs are the regions selectively engaged in M-pathway (IPS and SFG) and P-pathway (FG) processing by conducting a pilot study using functional localizer scans for M-pathway and P-pathway regions (Supplementary Result 7). In this pilot study, we used non-face stimuli, sinusoidal counter-phase flickering gratings biased to engage the M-pathway (a low-luminance contrast, varying grey-on-grey grating with a low spatial frequency and a 15 Hz flicker) and P-pathway (an isoluminant, high colour-contrast red-green grating with a high spatial frequency and a slow 5 Hz flicker), following the methods described by Denison et al.[84]. These types of stimuli have been known to selectively bias M-pathway and P-pathway processing in previous studies using object, letter, scene and face stimuli[44,45,50,84–87]. Although different types of stimuli and different cohorts of participants were employed, the localizer scans showed activations in foci adjacent to and overlapping with our ROIs, including the bilateral IPS and SFG activated by M-pathway stimuli and the bilateral FG activated by P-pathway stimuli.

Brain activations for comparing angry versus neutral crowds and neutral versus happy crowds. Our secondary interest was to examine the different patterns of brain activation when participants had to choose an angry over a neutral crowd (obvious and task-congruent comparison) versus choosing a neutral crowd over a happy crowd (less-obvious comparison). As shown in Fig. 5a, we found greater activations evoked by the avoidance comparison between an angry versus a neutral crowd in the brain areas along the dorsal visual pathway (the SFG, middle frontal gyrus, inferior frontal gyrus, supplementary motor area and orbitofrontal cortex), the ventrolateral PFC, PCC, amygdala and PHC in the RH, and the left superior parietal lobule (Fig. 5a). Overall, many of these regions overlapped

© 2017 Macmillan Publishers Limited, part of Springer Nature. All rights reserved.

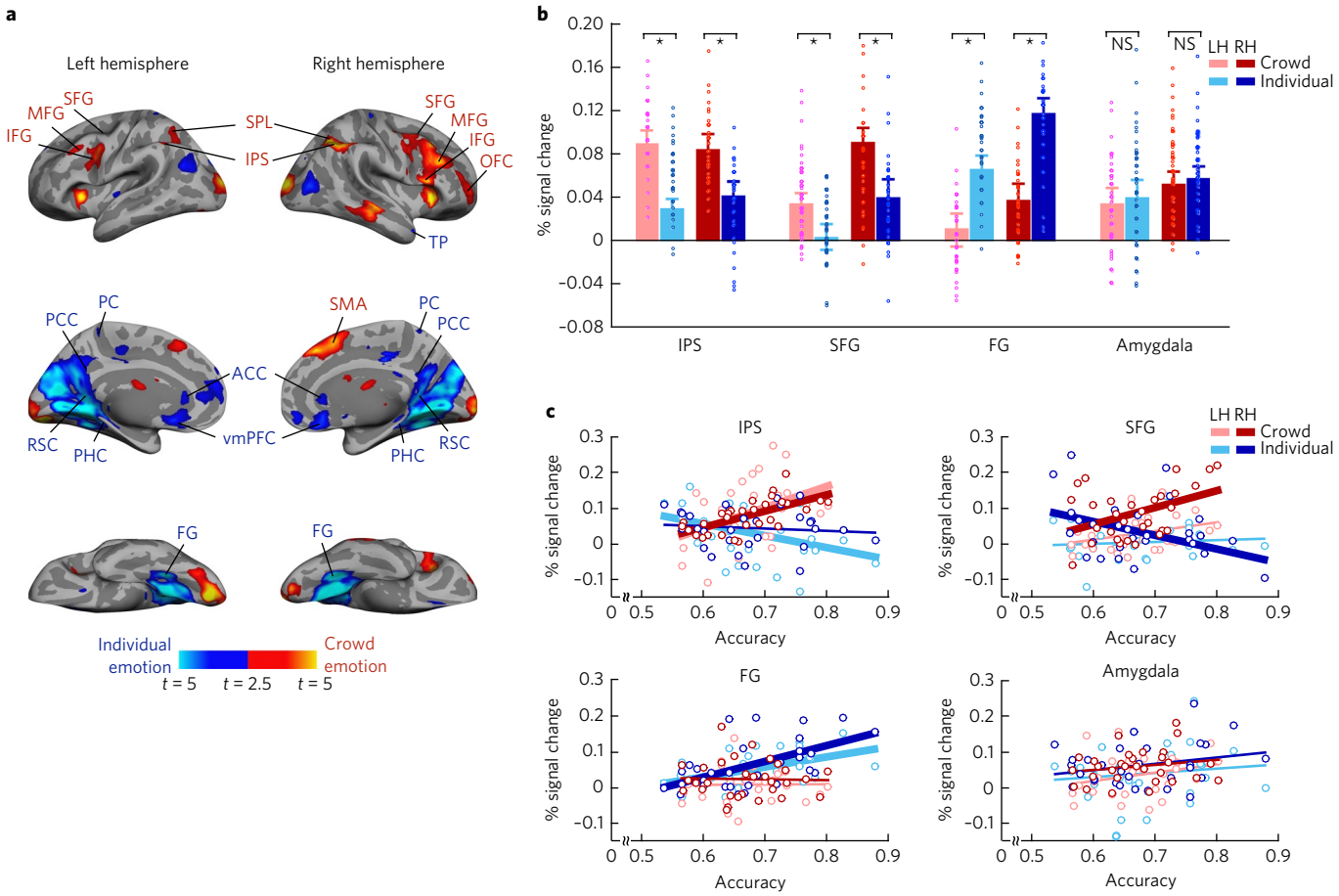

Fig. 4 | Distinct neural pathways preferentially involved in dorsal and ventral visual pathways for crowd emotion and individual emotion processing, respectively. a, The brain areas that showed greater activation when participants were making avoidance decisions by comparing two crowds are shown in red and the brain areas that showed greater activation when participants compared two single faces are shown in blue. The activations were thresholded at $P < 0.05$, family-wise error-corrected. The complete list of activations is labelled and reported in Table 1 and the results of the same contrasts at different thresholds are reported in Supplementary Tables 1 and 2. ACC, anterior cingulate cortex; FG, fusiform gyrus; IFG, inferior frontal gyrus; IPS, intraparietal sulcus; MFG, middle frontal gyrus; OFC, orbitofrontal cortex; PHC, parahippocampal cortex; PC, precuneus; PCC, posterior cingulate cortex; RSC, retrosplenial cortex; SFG, superior frontal gyrus; SMA, supplementary motor area; SPL, superior parietal lobule; TP, temporal pole; vmPFC, ventromedial prefrontal cortex. **b**, Percent signal change in the ROIs (the bilateral IPS, SFG, FG and amygdala) when participants were making avoidance decisions by comparing two crowds (pink and red bars for the LH and RH, respectively) and two single faces (light and dark blue bars for the LH and RH, respectively). The points represent data from individual participants. NS, not significant. The error bars indicate the standard error of the mean (s.e.m.) and the asterisks represent $P < 0.05$. **c**, Correlation between the percent signal change and the participants' accuracy for the crowd emotion condition (pink and red dots for the LH and RH, respectively) and the individual emotion condition (light and dark blue dots for the LH and RH, respectively), with overlaid linear regression lines in the same colours. The thick regression lines indicate statistically significant correlations (at $P < 0.05$) between the individual participants' accuracy and the percent signal change of each ROI.

with the areas showing preference for crowd emotion over individual emotion processing (Fig. 4a and Table 1), suggesting that task-congruent decision is dominant in the crowd emotion processing of these dorsal pathway regions. For the avoidance comparison between a neutral versus a happy crowd, we observed greater activations in the bilateral middle temporal gyrus and the SFG, superior temporal sulcus, PCC, PHC, ACC and medial PFC in the LH. Some of these areas, including the middle temporal gyrus, PCC and ACC, are also known to be engaged in emotional conflict resolution, coupled with the dorsolateral PFC, which is responsible for integration of emotional and affective processes[88–90]. Thus, this result suggests that choosing a neutral versus a happy crowd as a relative option to be avoided may engage an additional control mechanism. The control mechanism in these areas appears to be responsible for resolution of possible emotional conflict between the task goal (for example, avoidance) and the motivational value elicited by a happy facial crowd (for example, approach). The complete list of the brain activations in Fig. 5a is shown in Supplementary Table 3. Finally, comparing an angry versus a neutral face evoked greater activation in brain areas, including the bilateral angular gyrus, middle temporal gyrus, PHC, PCC/precuneus, right temporal pole, PFC and orbitofrontal cortex, whereas comparing a neutral versus a happy face evoked greater activation in areas including the left inferior frontal gyrus, insula, temporal pole and supplementary motor area (shown in Fig. 5b). A complete list of the brain activations in Fig. 5b is shown in Supplementary Table 4.

Discussion

The goal of this study was to characterize the functional and neural mechanisms that support crowd emotion processing. There were four main findings: (1) goal-dependent hemispheric asymmetry for crowd emotion processing, in which presenting a facial crowd to be chosen (for example, either an angry or a neutral crowd for the avoidance task and either a happy or a neutral crowd for the

© 2017 Macmillan Publishers Limited, part of Springer Nature. All rights reserved.

Table 1 | Significantly activated areas in mean responses for crowd emotion minus individual emotion and individual emotion minus crowd emotion contrasts

Activation location	MNI coordinates			*t* value	Extent
	x	*y*	*z*		
Crowd emotion > individual emotion					
Left visual cortex (BA18)	−15	−88	−14	7.281	1,210
	−21	−97	14	4.998	–
Left visual cortex (BA19)	−33	−79	−16	3.888	–
Right visual cortex (BA18)	18	−100	12	5.858	666
Right superior frontal gyrus	33	8	64	5.686	3,428
Right middle frontal gyrus	36	32	46	6.267	–
Left superior frontal gyrus	−24	9	64	3.112	46
Left middle frontal gyrus	−42	26	38	3.067	380
	−42	50	26	3.024	91
	−42	56	7	3.098	–
Right anterior insula	30	26	2	5.864	3,428
Left anterior insula	−33	20	4	5.858	176
Right intraparietal sulcus	39	−58	48	5.607	967
Right superior parietal lobule	36	−64	52	5.051	–
Left intraparietal sulcus	−39	−49	38	4.677	368
Right superior temporal sulcus	48	−25	−10	4.709	404
Left superior temporal sulcus	−54	−43	−8	3.303	26
Right supramarginal gyrus	54	−46	32	2.556	967
Left supramarginal gyrus	−51	−52	56	2.774	368
	−51	−43	3	2.928	9
Right cerebellum	33	−52	−44	2.876	15
Left cerebellum	−33	−55	−42	3.901	178
Right supplementary motor area	9	32	48	5.000	511
Left superior parietal lobule	−30	−67	48	3.477	368
Left premotor cortex	−39	5	36	4.364	380
Left inferior frontal gyrus	−27	26	22	3.586	21
Right caudate	12	20	6	3.046	18
Right brainstem	9	−16	−8	2.804	13
Individual emotion > crowd emotion					
Right visual cortex (BA19)	12	−64	−8	8.054	5,336
Right fusiform gyrus	27	−55	−14	5.998	–
Right parahippocampal cortex	21	−43	−10	4.943	–
Right retrosplenial cortex	18	−61	12	4.891	–
Left visual cortex (BA19)	−18	−55	−6	6.742	5,336
Left fusiform gyrus	−27	−46	−12	5.699	–
Left parahippocampal cortex	−27	−43	−10	5.623	–
Left primary visual cortex (BA17)	−6	−73	6	6.421	–
Left retrosplenial cortex	−18	−55	4	5.281	–
Left posterior cingulate cortex	−9	−52	32	−2.858	–
Right posterior cingulate cortex	12	−25	42	4.384	91
Right temporal pole	51	17	−39	4.564	34
	27	14	−32	2.849	8
	42	8	−28	3.239	9
Left precuneus	−12	−43	60	3.258	71
	−6	−61	66	2.796	8
Right precuneus	6	−52	64	2.863	26
Right visual cortex (BA19)	48	−79	16	4.246	272
Left ventromedial prefrontal cortex	−18	14	−22	3.581	23
Right ventromedial prefrontal cortex	9	26	−12	4.031	406
	9	47	−8	3.452	374
Left middle cingluate cortex	−12	−28	40	3.222	65
Right middle cingulate cortex	6	−13	44	2.992	15
Anterior cingulate cortex	0	32	6	3.446	406
Left angular gyrus	−42	−67	24	3.594	228
	−18	14	−22	3.336	23
Left posterior insula	−39	−16	0	3.346	28
Left insula	−42	2	6	2.994	11
Right posterior insula	44	−4	−8	3.172	58
Left medial prefrontal cortex	−12	47	40	2.731	374
Left supramarginal gyrus	−57	−37	28	3.251	40
Right hippocampus	27	−13	−22	2.871	16
Left orbitofrontal cortex	−45	29	−8	2.804	6

The activations were thresholded at $P < 0.05$, family-wise error-corrected. An en rule indicates that this cluster is part of a larger cluster immediately above.

approach task) in the LVF/RH facilitated participants' accuracy, (2) higher accuracy overall in identifying facial crowds containing task-congruent crowd emotion (for example, angry crowd to avoid or happy crowd to approach), (3) higher accuracy when sex-linked identity cues were congruent with the task goal (for example, angry male crowds to avoid and happy female crowds to approach) and (4) a preferentially activated dorsal visual stream in crowd emotion processing, with the IPS and SFG predicting behavioural crowd emo-

© 2017 Macmillan Publishers Limited, part of Springer Nature. All rights reserved.

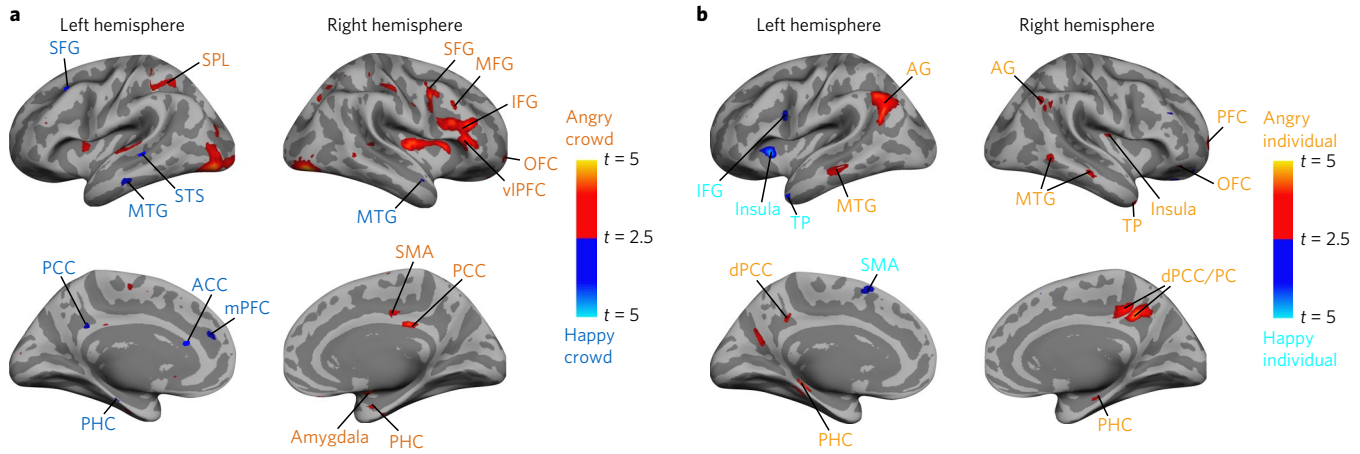

Fig. 5 | Brain activations by different types of avoidance comparisons. a, Brain areas that showed greater activation when participants were making avoidance decisions by comparing an angry crowd versus a neutral crowd (red labels) and brain areas that showed greater activation when participants compared a neutral crowd versus a happy crowd (blue labels). **b**, Brain areas that showed greater activation when participants were making avoidance decisions by comparing an angry face versus a neutral face (orange labels) and brain areas that showed greater activation when participants compared a neutral face versus a happy face (cyan labels). ACC, anterior cingulate cortex; AG, angular gyrus; dPCC, dorsal posterior cingulate cortex; IFG, inferior frontal gyrus; MFG, middle frontal gyrus; mPFC, medial prefrontal cortex; MTG, middle temporal gyrus; OFC, orbitofrontal cortex; PC, precuneus; PCC, posterior cingulate cortex; PFC, prefrontal cortex; PHC, parahippocampal cortex; SFG, superior frontal gyrus; SMA, supplementary motor area; SPL, superior parietal lobule; STS, superior temporal gyrus; TP, temporal pole; vlPFC, ventrolateral prefrontal cortex.

tion efficiency, and a preferentially activated ventral visual stream in individual face emotion processing, with fusiform cortex activity predicting the accuracy of decisions about individual face emotion.

The goal-dependent modulation of crowd emotion processing suggests that the mechanism underlying the reading of crowd emotion is highly flexible and adaptive, allowing perceivers to focus most keenly on desired outcomes in dynamic social contexts (for example, to avoid unfriendly crowds or to approach friendly ones). Neither the stimulus display nor the response characteristics changed between avoidance and approach tasks: the only difference was the decision (approach or avoid) that was mapped to the response. The same visual stimuli containing facial crowds appeared to be biased differently depending on whether the task goal was to avoid or to approach. Stimulus gender also interacted with the processing of crowd emotion in a manner relevant to the current goal. Such visual integration of compound social cues (for example, gender, emotion, race, eye gaze, body language, and so on) has been well incorporated into the theories of mechanisms underlying single face perception[91]. However, the roles of these compound social cues in ensemble coding of facial crowds have not been examined. The current study provides evidence that intrinsic (social motivation shaped by the task instruction in this study) and extrinsic factors (for example, emotional expressions and the sex of the individuals in the crowds) also mutually facilitate the reading of crowd emotion in a manner that is functionally related to the task at hand. Future studies will be needed to further explore how other relevant information about environment and context modulates perception of crowd emotion and individual emotion differently and how perceived crowd and individual emotion yield different emotional intensity and confidence of observers in order to initiate an appropriate social response toward it.

Our findings also provide evidence that the processing that supports social decisions on crowd emotions is highly lateralized in a manner that is relevant to the current task goal. Lateralized behavioural responses provide an opportunity to study the hemispheric asymmetries that enable cognitive functions. This hemispheric asymmetry enables flexible and adaptive processing optimized for the current task goal in dynamic environments[92], supporting the selection of appropriate—and inhibition of inappropriate—responses[93]. This is particularly useful when a large number of complex stimuli (such as a crowd of emotional faces) and competing cognitive goals tax the processing capacity of the visual system, as was the case in our task. The pattern of hemispheric lateralization in affective processing has been traditionally thought to rely on emotional valence[35,94], with aversive or negative stimuli lateralized to the RH and positive, approach-evoking stimuli lateralized to the LH. However, we instead found that the lateralization effects in crowd emotion processing are goal dependent, rather than being driven purely by stimulus valence. Our findings demonstrate that the same emotional stimuli can be biased differently in the RH and LH, depending on the task goal and observer's intent. Specifically, the current task goal (approach or avoidance) biased processing such that the LVF/RH was superior for recognizing a 'relatively angrier' facial crowd during the avoidance task and for processing a 'relatively happier' facial crowd during the approach task. Since the task-relevant emotions were anger and happiness for the avoidance and approach tasks, respectively, our results suggest that global processing of ensemble face emotion most strongly engages the RH in general, consistent with a popular concept of the dominant role of RH in global processing[75–79]. Unlike the crowd emotion condition, however, we observed a RH advantage for an angry face and a LH advantage for a neutral face. This also conforms to the traditional framework of single face processing, with RH preference for aversive or negative face stimuli and LH preference for positive, approach-evoking stimuli[31,35,82,95]. Together, our data suggest that reading crowd emotion and single face emotion leads to different patterns of hemispheric lateralization, with crowd emotion processing showing flexible modulation of the RH dominance depending on the task goal, rather than being based purely on stimulus valence.

It is worth noting that the inference should be made very carefully from the divided visual field paradigm because it is a relatively indirect approach to localizing hemispheres with cognitive functions[96]. In particular, the interpretation of the results becomes very difficult when participants shift their gaze. To ensure that participants did not move their eyes while they performed the current task, we explicitly instructed participants to initiate each trial only after they fixated the central fixation cross. Moreover, we verified from the

© 2017 Macmillan Publishers Limited, part of Springer Nature. All rights reserved.

control eye-tracking experiment (control experiment 2) that we could replicate our results from the main experiments (1a and 2) when participants' eye movements were monitored and restricted (Supplementary Result 4). Finally, we also replicated this hemispheric lateralization for crowd emotion processing in all the main and control experiments (see Supplementary Result 6). Therefore, we conclude that our results are robust to confounding factors such as variability in facial stimuli, differences in experimental settings (behavioural, eye-tracking and fMRI), and participants' eye movements and variability across different cohorts of participants.

For a given pair of facial crowds to be compared in our study, participants were asked to choose which one of the two should be avoided (avoidance task) or approached (approach task) relatively more. Although both an angry crowd compared with a neutral crowd and a neutral crowd compared with a happy crowd showed a RH advantage during the avoidance task, these two different types of comparisons may have yielded a different amount of emotional ambiguity and task difficulty. In our fMRI study, we found greater activations evoked by goal-congruent comparison (an angry versus a neutral crowd) in the brain areas along the dorsal visual pathway (the SFG, middle frontal gyrus, inferior frontal gyrus, supplementary motor area and orbitofrontal cortex), as well as in the ventrolateral PFC, PCC, amygdala and PHC in the RH, and in the left superior parietal lobule. This result suggests that task-congruent decisions may occur predominantly in the crowd emotion processing of these dorsal pathway regions, with the RH more pronounced. However, when comparing a neutral versus a happy crowd, we observed greater activations in the bilateral middle temporal gyrus and the left SFG, superior temporal sulcus, PCC, PHC, ACC and medial PFC. The middle temporal gyrus, PCC and ACC are known to be engaged in emotional conflict resolution, coupled with the dorsolateral PFC, which is responsible for integration of emotional and affective processes[19,88,89]. When a goal-incongruent emotional stimulus interferes with a goal-congruent emotional stimulus, emotional conflict occurs[97]. Thus, this finding suggests that choosing a neutral over a happy crowd during the avoidance task may involve an emotional conflict control mechanism[98,99] in which possible interference by a goal-incongruent facial crowd (for example, a happy crowd) is suppressed and the ambiguity of a neutral crowd is resolved as a relatively better option for the avoidance decision.

Different patterns of hemispheric lateralization for the crowd emotion versus individual emotion processing suggest that they may rely on qualitatively distinct systems. Much behavioural evidence has been accumulated supporting this notion[6,7,11–15,21,100–104] (but see ref. [105]), although only a few recent fMRI studies have compared the neural representations of ensemble coding and individual processing[106–108]. Cant and Xu[106,107] showed that the parahippocampal place area and lateral occipital cortex were preferentially engaged in texture perception and object processing, respectively, and Huis In 't Veld and de Gelder[108] showed greater anticipatory and action preparation activity in areas including the inferior parietal lobule, superior parietal lobule, SFG and premotor cortex for interactive body movement in a group of panicked people compared with an unrelated movement of individuals. However, unlike previous work that used stimuli of simple texture patches and objects[106,107] or removed the information about facial expressions of people from their blurred video clips[108], the current study examined the distinct neutral substrates underlying the processing of facial crowds with varying emotional expressions compared with the processing of individual emotion expressions, providing evidence for distinct mechanisms supporting them.

The benefit of having distinct systems for ensemble coding and individual object processing is that these two processes can serve complementary functions. Global information extracted via ensemble coding influences the processing of individual objects in many different ways. Because ensemble coding compresses the properties of multiple objects into a compact description with a higher level of abstraction[109], it allows observers to surmount the severe limitations on individual object processing[110–114] imposed by attention or working memory[115–118]. Furthermore, the global information of ensembles allows for an initial, rough analysis of visual inputs, which then biases and facilitates the processing of individual objects[109,110,114,119]. For example, extracted ensemble representation influences individual object processing by guiding the detection of outliers in a set (for example, a pop-out visual search[109,119]), facilitating the selection of an individual object at the centre location of a set[114] and biasing memory for individual objects towards the global mean[120]. Our results from the whole-brain and the ROI analyses support our hypothesis that the dorsal visual stream contributes to global processing for crowd emotion extraction, whereas the ventral visual stream contributes more to object-based (local) processing of emotion in individual faces.

Processing of crowd emotion appears to be achieved in a global, parallel fashion, rather than serially for the following reasons. First, we found that the RTs for the crowd emotion condition were equivalent to those for the individual emotion, despite the many more faces that needed to be processed in the crowd condition compared with the individual face condition (see Supplementary Result 8). Second, simply sampling any one or two individual faces from each crowd in our stimuli would have led to the chance level of accuracy, because half of the individual members in the neutral crowd were always more intense than half of the angry crowd in our stimuli. Thus, sampling faces with an extreme emotional expression would not explain our findings. Third, the participants were equally accurate and fast when they viewed the facial crowds containing 8 faces or 12 faces. Finally, fixating eyes to the centre did not impair participants' accuracy or RT for extracting crowd emotion, indicating that making saccades towards individual faces in the crowd to foveate them is not essential to effectively evaluate crowd emotion in our task. Therefore, we suggest that extracting crowd emotion relies on a parallel, global process, rather than on sequential sampling of individual members[105]. In various feature dimensions, the notion of global averaging has been previously tested, using empirical approaches showing that multiple stimuli were integrated[22], ideal observer analysis[3,15], equivalent noise[26] or general linear modelling[17]. Consistent with this previous work, the current findings suggest that people average different facial expressions to make social decisions about facial crowds and that such ensemble coding of crowds of faces is achieved via a mechanism distinct from that supporting individual object processing.

To conclude, we report evidence for distinct mechanisms dedicated to processing crowd emotion and individual face emotion, which are biased towards different visual streams (dorsal versus ventral) and show different patterns of hemispheric lateralization. The differential engagement of the dorsal stream regions and the complementary functions of the LH and RH both suggest that processing of crowd emotion is specialized for action execution that is highly flexible and goal driven, allowing us to trigger a rapid and appropriate reaction to our social environment. Furthermore, we have shown that observers' goals—to avoid or approach—can exert powerful influences on the perception accuracy of crowd emotion, highlighting the importance of understanding the interplay of ensemble coding of crowd emotion and social vision.

Methods

Participants. A total of 42 undergraduate students participated in experiment 1: 21 subjects (12 female) participated in the avoidance task (experiment 1a) and a different cohort of 21 participants (11 female) participated in the approach task (experiment 1b). A power analysis[121] based on a pilot run of this experiment with four subjects indicated that 21 subjects was sufficient to achieve at least 80% power. No subjects were excluded from the behavioural data analysis. A new group of 32 (18 female) undergraduate students participated in experiment 2. Two participants

© 2017 Macmillan Publishers Limited, part of Springer Nature. All rights reserved.

were excluded from further analyses because they made too many late responses (for example, their RTs were longer than 2.5 s). Thus, the behavioural and fMRI analyses for experiment 2 were performed with a sample of 30 participants. All the participants had normal colour vision and normal or corrected-to-normal visual acuity. Informed written consent was obtained according to the procedures of the Institutional Review Board at the Pennsylvania State University. The participants received monetary compensation or a course credit.

Apparatus and stimuli. Stimuli were generated using MATLAB and the Psychophysics Toolbox[122,123]. In each crowd stimulus (Fig. 1a), either four or six morphed faces were randomly positioned in each visual field (right and left) on a grey background. Therefore, our facial crowd stimuli comprised either 8 or 12 faces. We used face-morphing software (Norrkross MorphX version 2.14; www.norrkross.com/software/morphx/morphx.php) to create a set of 51 morphed faces from two highly intense, prototypical facial expressions of the same person for a set of six different identities (three male and three female faces), taken from the Ekman face set[69]. The morphed face images were controlled for luminance, and the emotional expression of the faces ranged from happy to angry (Fig. 1a), with 0 emotional units being neutral (a morph of 50% happy and 50% angry), +25 emotional units being the happiest (100% happy) and −25 emotional units being the angriest (100% angry). As the morphed face images were linearly interpolated (in 2% increments) between two extreme faces, they were separated from one another by emotional units of intensity such that face 1 was one emotional unit happier than face 2, and so on. Therefore, the larger the separation between any two morphed faces in emotional units, the easier it was to discriminate between them. Such a morphing approach was adapted from previous studies on ensemble coding of faces[16].

Since the previous literature on averaging of other visual features showed that the range of variation is an important determinant of averaging performance (for example, size or hue[124,125]), we kept the range of faces the same (that is, 18 emotional units) across the two set sizes. This number of emotional units was determined from initial pilot work to ensure that each individual face was distinguishable from the others in the range and that the task was not so easy as to produce accuracy ceiling effects. One of the two crowds in either the LVF or RVF always had a mean value of 0 emotional units, which was neutral on average, and the other had an emotional mean of +9 (very happy; morphing of angry 32% and happy 68%), +5 (somewhat happy; morphing of angry 40% and happy 60%), −9 (very angry; morphing of angry 68% and happy 32%) or −5 (somewhat angry; morphing of angry 60% and happy 40%). Thus, the sign of such offset between the emotional and neutral crowds in emotional units indicates the valence of the emotional crowd compared with the neutral. The positive values indicate a more positive (happier) crowd emotion compared with the neutral and the negative values indicate a more negative (angrier) mean emotion.

To avoid the possibility that participants simply sampled one or two single faces from each set and compared them to perform the crowd emotion task, we ensured that 50% of the individual faces in the neutral set were more expressive than 50% of the individual faces in the emotional sets to be compared. For example, half of the members of the neutral set were angrier than half of the members of the angry crowd. This manipulation allowed us to assess whether participants used such a sampling strategy[105] rather than extracting an average, because sampling one or two members in a set would yield 50% accuracy in this setting.

Stimuli for the individual emotion condition (Fig. 1c; only included in the fMRI study) comprised one emotional face (either angry or happy) and one neutral face from the same set of morphed face images randomly positioned in the same invisible frame surrounding the crowd stimuli in each visual field. The offsets between the emotional and neutral faces remained the same as those in the facial crowd stimuli. To ensure that the difference was not due to the confound of simply having more 'stuff' in the crowd emotion condition compared with the individual emotion condition, we included scrambled faces in the individual emotion condition so that the same number of face-like blobs were presented as in the crowd emotion condition. This ensured that any differences are not due to low-level visual differences in the stimulus displays, but rather to how many resolvable emotional faces participants had to discriminate on each trial (2 versus 8 or 12).

In one half of the trials, the emotional stimulus (that is, happy or angry: ±5 or ±9 emotional units away from the mean) was presented in the LVF and the neutral stimulus was presented in the RVF, and this was switched for the other half of the trials. Each face image subtended 2°×2° of the visual angle, and face images were randomly positioned within an invisible frame subtending 13.29°×18.29°, each in the LVF and RVF. The distance between the proximal edges of the invisible frames in LVF and RVF was 3.70°.

Procedure. Participants in experiment 1 sat in a chair in individual cubicles 61 cm away from a computer with a 48 cm diagonal screen (refresh rate = 60 Hz). Participants in experiment 2 were presented with the stimuli rear-projected onto a mirror attached to a 64-channel head coil in the fMRI scanner. Figure 1b illustrates a sample trial of the experiment. Participants were presented with visual stimuli for 1 s, followed by a blank screen for 1.5 s. The participants were instructed to make a key press as soon as possible to indicate which of the two crowds of faces or two single faces on the left or right they would rather avoid (experiment 1a and experiment 2) or approach (experiment 1b). Participants pressed the 'f' key when choosing the LVF and 'j' key when choosing the RVF in the behavioural experiments (1a and 1b). In the fMRI scanner experiment (2), they pressed the '1' key for the LVF and the '4' key for the RVF using a button box. They used both left and right index fingers. Key-response assignment was not counterbalanced to maintain the automatic and consistent stimulus-response compatibility[126] (left key for the LVF and right key for the RVF). They were explicitly informed that the correct answer was to choose either the crowd or the face showing a more negative (for example, angrier) emotion for the avoidance task and a more positive (for example, happier) emotion for the approach task. Responses that were made after 2.5 s were considered late and excluded from the data analyses. Feedback for correct, incorrect or late responses was provided after each response. Before the experiment session began, participants were provided with 20 practice trials that were conceptually identical to the actual trials.

In experiment 1, half of the participants performed the avoidance task and the other half performed the approach task. Experiment 1 had a 4 (emotional distance between facial crowds: −9, −5, +5 or +9) ×2 (visual field of presentation: LVF or RVF) ×2 (set size: 4 or 6 faces in each visual field) design, and the sequence of a total of 320 trials (20 repetitions per condition) was randomized. In experiment 2 (fMRI), all the participants performed the avoidance task. Because we needed more trials for statistical power for the fMRI data analyses and we observed no effect by the number of crowd members on crowd emotion perception (Supplementary Fig. 1), we only used crowd stimuli containing 4 faces in experiment 2. Thus, experiment 2 had a 2 (stimulus type: crowd or individual) ×4 (emotional distance) ×2 (visual field of presentation) design and 112 additional null trials (background trial without visual stimulation). The sequence of a total of 624 trials including 512 experimental trials (32 repetitions per condition) and 112 null trials was optimized for haemodynamic response estimation efficiency using the optseq2 software (https://surfer.nmr.mgh.harvard.edu/optseq/).

fMRI data acquisition and analysis. The fMRI images of brain activity were acquired using a 3T scanner (Magnetom Prisma; Siemens) located at the Pennsylvania State University Social, Life, and Engineering Sciences Imaging Center. High-resolution anatomical MRI data were acquired using T1-weighted images for the reconstruction of each subject's cortical surface (repetition time = 2,300 ms, echo time = 2.28 ms, flip angle = 8°, field of view = 256×256 mm^2, slice thickness = 1 mm, sagittal orientation). The functional scans were acquired using gradient-echo echo-planar imaging with a repetition time of 2,000 ms, an echo time of 28ms, a flip angle of 52° and 64 interleaved slices (3×3×2 mm). Scanning parameters were optimized by manual shimming of the gradients to fit the brain anatomy of each subject, and tilting the slice prescription anteriorly 20–30° up from the anterior commissure–posterior commissure line, as described in previous studies[44,127,128] to improve the signal and minimize susceptibility artefacts in the brain regions including the orbitofrontal cortex and amygdala[129]. We acquired 780 functional volumes per subject in four functional runs, each lasting 6.5 min.

The acquired fMRI mages were pre-processed using SPM8 (Statistical Parametric Mapping, Wellcome Department of Cognitive Neurolgy).

The functional images were corrected for differences in slice timing, realigned, corrected for movement-related artefacts, co-registered with each participant's anatomical data, normalized to the Montreal Neurological Institute template and spatially smoothed using an isotropic 8 mm full width half-maximum Gaussian kernel. Outliers due to movement or signal from preprocessed files, using thresholds of 3 standard deviations from the mean, 0.75 mm for translation and 0.02 radians rotation, were removed from the data sets using the ArtRepair software[130]. Subject-specific contrasts were estimated using a fixed-effects model. These contrast images were used to obtain subject-specific estimates for each effect. For group analyses, these estimates were then entered into a second-level analysis treating participants as a random effect, using one-sample *t*-tests at each voxel. Six contrasts of interest were used: (1) crowd emotion minus individual emotion, (2) individual emotion minus crowd emotion, (3) angry crowd minus happy crowd, (4) happy crowd minus angry crowd, (5) angry individual minus happy individual and (6) happy individual minus angry individual. These contrasts were thresholded at $P < 0.05$ (family-wise error whole-brain corrected) and a minimum cluster size of five voxels. For visualization and anatomical labelling purposes, all group contrast images were overlaid onto the inflated group average brain using two-dimensional surface alignment techniques implemented in FreeSurfer[131].

For the ROI analyses, we extracted the blood-oxygen-level dependent activity from the bilateral IPS, SFG, FG and amygdala. We defined a separate contrast between all the visual stimulation trials (all trials containing stimuli) versus background (null trials). From this contrast, we localized each of the ROIs based on the peak activation within the anatomical label obtained by the anatomical parcellation of the normalized brain[83]. The L/R *x*, *y*, *z* coordinates for these ROIs were −30/30, −67/−70, 52/42 for the IPS, −27/36, 5/6, 66/58 for the SFG, −30/33, −58/−58, −10/−10 for the FG and −18/18, −1/−4, −18/−12 for the amygdala. The coordinates for the right IPS and the right SFG were adjacent to the regions that have been reported in a previous study to show the robust intra-stream connectivity (dorsal visual stream[56]). Moreover, the coordinate for the right

© 2017 Macmillan Publishers Limited, part of Springer Nature. All rights reserved.

FG has also been localized as the right fusiform face area in the activation maps by Spiridon, Fischl and Kanwisher[132]. The beta weights were extracted for crowd emotion and individual emotion conditions using the rfxplot toolbox (http://rfxplot.sourceforge.net) for SPM. We defined a 6 mm sphere around the *x*, *y*, *z* coordinate for each of our ROIs. Using the rfxplot toolbox in SPM 8, we extracted all the voxels from each individual participant's functional data within that sphere. To achieve our main goal of mapping out the brain regions that are preferentially engaged in crowd emotion processing versus individual emotion processing, we collapsed the four different levels of emotional distance (−9, −5, +5 and +9) and the two levels of visual field of presentation (LVF and RVF). On the extracted beta estimates for the two main conditions (crowd emotion and individual emotion) from each of the ROIs, we conducted paired *t*-tests to compare the percent signal change between the crowd emotion versus individual emotion conditions and the correlation analyses to examine the relationship with the behavioural accuracy measurements. In Supplementary Fig. 10, we also report the beta estimates from the breakdown of the emotional valence for crowd emotion and individual emotion conditions (four conditions in total: angry crowd, happy crowd, angry individual and happy individual).

Code availability. All the MATLAB codes for the behavioural and fMRI analyses presented in this study are available from H.Y.I. (him3@mgh.harvard.edu) or the corresponding author on request.

Data availability. The datasets generated and/or analysed during the current study are available from H.Y.I. or the corresponding author on reasonable request.

Received: 27 January 2017; Accepted: 11 September 2017;
Published online: 09 October 2017

References

1. Alvarez, G. A. Representing multiple objects as an ensemble enhances visual cognition. *Trends Cogn. Sci.* **15**, 122–131 (2011).
2. Fischer, J. & Whitney, D. Object-level visual information gets through the bottleneck of crowding. *J. Neurophysiol.* **106**, 1389–1398 (2011).
3. Haberman, J., Harp, T. & Whitney, D. Averaging facial expression over time. *J. Vis.* **9**, 1–13 (2009).
4. Haberman, J. & Whitney, D. Efficient summary statistical representation when change localization fails. *Psychon. Bull. Rev.* **18**, 855–859 (2011).
5. Dakin, S. C. & Watt, R. J. The computation of orientation statistics from visual texture. *Vision Res.* **37**, 3181–3192 (1997).
6. Parkes, L., Lund, J., Angelucci, A., Solomon, J. A. & Morgan, M. Compulsory averaging of crowded orientation signals in human vision. *Nat. Neurosci.* **4**, 739–744 (2001).
7. Ariely, D. Seeing sets: representation by statistical properties. *Psychol. Sci.* **12**, 157–162 (2001).
8. Chong, S. C. & Treisman, A. Representation of statistical properties. *Vision Res.* **43**, 393–404 (2003).
9. Watamaniuk, S. N. J. & Sekuler, R. Temporal and spatial integration in dynamic random-dot stimuli. *Vision Res.* **32**, 2341–2347 (1992).
10. Halberda, J., Sires, S. F. & Feigenson, L. Multiple spatially overlapping sets can be enumerated in parallel. *Psychol. Sci.* **17**, 572–576 (2006).
11. Alvarez, G. A. & Oliva, A. The representation of simple ensemble visual features outside the focus of attention. *Psychol. Sci.* **19**, 392–398 (2008).
12. Choo, H. & Franconeri, S. L. Objects with reduced visibility still contribute to size averaging. *Atten. Percept. Psychophys.* **72**, 86–99 (2010).
13. Corbett, J. E. & Oriet, C. The whole is indeed more than the sum of its parts: Perceptual averaging in the absence of individual item representation. *Acta Psychol.* **138**, 289–301 (2011).
14. Haberman, J. & Whitney, D. The visual system discounts emotional deviants when extracting average expression. *Atten. Percept. Psychophys.* **72**, 1825–1838 (2010).
15. Im, H. Y. & Halberda, J. The effects of sampling and internal noise on the representation of ensemble average size. *Atten. Percept. Psychophys.* **75**, 278–286 (2013).
16. Haberman, J. & Whitney, D. Rapid extraction of mean emotion and gender from sets of faces. *Curr. Biol.* **17**, R751–R753 (2007).
17. Hubert-Wallander, B. & Boynton, G. M. Not all summary statistics are made equal: evidence from extracting summaries across time. *J. Vis.* **15**, 1–12 (2015).
18. Ji, L., Chen, W. & Fu, X. Different roles of foveal and extrafoveal vision in ensemble representation for facial expressions. *EPCE* **8532**, 164–173 (2014).
19. Yang, J.-W., Yoon, K. L., Chong, S. C. & Oh, K. J. Accurate but pathological: social anxiety and ensemble coding of emotion. *Cog. Ther. Res.* **37**, 572–578 (2013).
20. De Fockert, J. W. & Wolfenstein, C. Rapid extraction of mean identity from sets of faces. *Q. J. Exp. Psychol.* **62**, 1716–1722 (2009).
21. Leib, A. Y., Puri, A. M., Fischer, J., Bentin, S., Whitney, D. & Robertson, L. Crowd perception in prosopagnosia. *Neuropsychologia* **50**, 1698–1707 (2012).
22. Leib, A. Y., Fischer, J., Liu, Y., Qiu, S., Robertson, L. & Whitney, D. Ensemble crowd perception: a viewpoint-invariant mechanism to represent average crowd identity. *J. Vis.* **14**, 1–13 (2014).
23. Neumann, M. F., Schweinberger, S. R. & Burton, A. M. Viewers extract mean and individual identity from sets of famous faces. *Cognition* **128**, 56–63 (2013).
24. Brunyé, T. T., Howe, J. L. & Mahoney, C. R. Seeing the crowd for the bomber: spontaneous threat perception from static and randomly moving crowd simulations. *J. Exp. Psychol. Appl.* **20**, 303–322 (2014).
25. Sweeny, T. D., Haroz, S. & Whitney, D. Perceiving group behavior: sensitive ensemble coding mechanisms for biological motion of human crowds. *J. Exp. Psychol. Hum. Percept. Perform.* **39**, 329–337 (2013).
26. Florey, J., Clifford, C. W., Dakin, S. & Mareschal, I. Spatial limitations in averaging social cues. *Sci. Rep.* **6**, 32210 (2016).
27. Sweeny, T. D. & Whitney, D. Perceiving crowd attention: ensemble perception of a crowd's gaze. *Psychol. Sci.* **25**, 1903–1913 (2014).
28. Adams, R. B. Jr., Ambady, N., Macrae, C. N. & Kleck, R. E. Emotional expressions forecast approach-avoidance behavior. *Motiv. Emot.* **30**, 179–188 (2006).
29. Horstmann, G. What do facial expressions convey: feeling states, behavioral intentions, or action requests? *Emotion* **3**, 150–166 (2003).
30. Marsh, A. A., Ambady, N. & Kleck, R. E. The effects of fear and anger facial expressions on approach- and avoidance-related behaviors. *Emotion* **5**, 119–124 (2005).
31. Davidson, R. J. Anterior cerebral asymmetry and the nature of emotion. *Brain Cogn.* **20**, 125–151 (1992).
32. Elliot, A. J. Approach and avoidance motivation and achievement goals. *Educ. Psychol.* **34**, 169–189 (1999).
33. Adams, R. B. Jr., Hess, U. & Kleck, R. E. The intersection of gender-related facial appearance and facial displays of emotion. *Emot. Rev.* **7**, 5–13 (2015).
34. Bargh, J. A., Chen, M. & Burrows, L. Automaticity of social behavior: direct effects of trait construct and stereotype activation on action. *J. Pers. Soc. Psychol.* **71**, 230–244 (1996).
35. Davidson, R. J. & Irwin, W. The functional neuroanatomy of emotion and affective style. *Trends Cogn. Sci.* **3**, 11–21 (1999).
36. De Renzi, E. Prosopagnosia in two patients with CT scan evidence of damage confined to the right hemisphere. *Neuropsychologia* **24**, 385–389 (1986).
37. Fabes, R. A. & Martin, C. L. Gender and age stereotypes of emotionality. *Pers. Soc. Psychol. Bull.* **17**, 532–540 (1991).
38. Kanwisher, N., McDermott, J. & Chun, M. M. The fusiform face area: a module in human extrastriate cortex specialized for face perception. *J. Neurosci.* **17**, 4302–4311 (1997).
39. Wada, Y. & Yamamoto, T. Selective impairment of facial recognition due to a haematoma restricted to the right fusiform and lateral occipital region. *J. Neurol. Neurosurg. Psychiatry* **71**, 254–257 (2001).
40. Merigan, W. H. & Maunsell, J. H. How parallel are the primate visual pathways? *Annu. Rev. Neurosci.* **16**, 369–402 (1993).
41. Sawatari, A. & Callaway, E. M. Convergence of magno- and parvocellular pathways in layer 4B of macaque primary visual cortex. *Nature* **380**, 442–446 (1996).
42. Freud, E., Plaut, D. C. & Behrmann, M. 'What' is happening in the dorsal visual pathway. *Trends Cogn. Sci.* **20**, 773–784 (2016).
43. Goodale, M. A. & Milner, A. D. Separate visual pathways for perception and action. *Trends Neurosci.* **15**, 20–25 (1992).
44. Kveraga, K., Boshyan, J. & Bar, M. The magnocellular trigger of top-down facilitation in object recognition. *J. Neurosci.* **27**, 13232–13240 (2007).
45. Kveraga, K., Ghuman, A. S. & Bar, M. Top-down predictions in the cognitive brain. *Brain Cogn.* **65**, 145–168 (2007).
46. Livingstone, M. S. & Hubel, D. E. Segregation of form, color, movement, and depth: anatomy, physiology, and perception. *Science* **240**, 740–749 (1988).
47. Milner, A. D. & Goodale, M. A. *The Visual Brain in Action* (Oxford Univ. Press, Oxford, 1995).
48. Milner, A. D. & Goodale, M. A. Two visual systems re-viewed. *Neuropsychologia* **46**, 774–785 (2008).
49. Schiller, P. H. & Logothetis, N. K. The color- opponent and broad-band channels of the primate visual system. *Trends Neurosci.* **13**, 392–398 (1990).
50. Thomas, C., Kveraga, K., Huberle, E., Karnath, H.-O. & Bar, M. Enabling global processing in simultanagnosia by psychophysical biasing of visual pathways. *Brain* **135**, 1578–1585 (2012).
51. Vuilleumier, P., Armony, J. L., Driver, J. & Dolan, R. J. Distinct spatial frequency sensitivities for processing faces and emotional expressions. *Nat. Neurosci.* **6**, 624–631 (2003).

© 2017 Macmillan Publishers Limited, part of Springer Nature. All rights reserved.

52. Winston, J. S., Vuilleumier, P. & Dolan, R. J. Effects of low-spatial frequency components of fearful faces on fusiform cortex activity. *Curr. Biol.* **13**, 1824–1829 (2003).
53. Courtney, S. M., Ungerleider, L. G., Keil, K. & Haxby, J. V. Object and spatial visual working memory activate separate neural systems in human cortex. *Cereb. Cortex* **6**, 39–49 (1996).
54. Courtney, S. M., Petit, L., Maisog, J. M., Ungerleider, L. G. & Haxby, J. V. An area specialized for spatial working memory in human frontal cortex. *Science* **279**, 1347–1351 (1998).
55. Sala, J. B. & Courtney, S. M. Binding of what and where during working memory maintenance. *Cortex* **43**, 5–21 (2007).
56. Takahashi, E., Ohki, K. & Kim, D.-S. Dissociation and convergence of the dorsal and ventral visual streams in the human prefrontal cortex. *Neuroimage* **65**, 488–498 (2013).
57. Wilson, F. A., Scalaidhe, S. P. & Goldman-Rakic, P. S. Dissociation of object and spatial processing domains in primate prefrontal cortex. *Science* **260**, 1955–1958 (1993).
58. Denys, K. et al. The processing of visual shape in the cerebral cortex of human and nonhuman primates: a functional magnetic resonance imaging study. *J. Neurosci.* **24**, 2551–2565 (2004).
59. Grill-Spector, K. & Malach, R. The human visual cortex. *Annu. Rev. Neurosci.* **27**, 649–677 (2004).
60. Haxby, J. V. et al. Dissociation of object and spatial visual processing pathways in human extrastriate cortex. *Proc. Natl Acad. Sci. USA* **88**, 1621–1625 (1991).
61. Purves, D. et al. *Neuroscience* 3rd edn (Sinauer Associates, Sunderland, MA, 2004).
62. Taylor, J. C., Wiggett, A. J. & Downing, P. E. Functional MRI analysis of body and body part representations in extrastriate and fusiform body parts. *J. Neurophysiol.* **98**, 1626–1633 (2007).
63. LeDoux, J. E. *The Emotional Brain* (Simon and Schuster, New York, NY, 1996).
64. Morris, J. S. et al. A differential neural response in the human amygdala to fearful and happy facial expressions. *Nature* **383**, 812–815 (1996).
65. Damasio, A. R. et al. Subcortical and cortical brain activity during the feeling of self-generated emotions. *Nat. Neurosci.* **3**, 1049–1056 (2000).
66. Vuilleumier, P., Armony, J. L., Driver, J. & Dolan, R. J. Effects of attention and emotion on face processing in the human brain: an event-related fMRI study. *Neuron* **30**, 829–841 (2001).
67. Zald, D. H. The human amygdala and the emotional evaluation of sensory stimuli. *Brain Res. Brain Res. Rev.* **41**, 88–123 (2003).
68. Whalen, P. J. et al. Human amygdala responsivity to masked fearful eye whites. *Science* **306**, 2061 (2004).
69. Ekman, P. & Friesen, W. V. *Pictures of Facial Affect* (Consulting Psychologists Press, Palo Alto, CA, 1976).
70. Botvinick, M. M., Cohen, J. D. & Carter, C. S. Conflict monitoring and anterior cingulate cortex: an update. *Trends Cogn. Sci.* **8**, 539–545 (2004).
71. Jonides, J. & Nee, D. E. Brain mechanisms of proactive interference in working memory. *Neuroscience* **139**, 181–193 (2006).
72. Monsell, S. Task switching. *Trends Cogn. Sci.* **7**, 134–140 (2003).
73. Rogers, R. D. & Monsell, S. The costs of a predictable switch between simple cognitive tasks. *J. Exp. Psychol. Gen.* **124**, 207–231 (1995).
74. Theios, J. in *Attention and Performance V* (eds Rabbitt, P. M. A. & Dornic, S.) 418–440 (Academic Press, New York, NY, 1975).
75. Christie, J., Ginsberg, J. P., Steedman, J., Fridriksson, J., Bonilha, L. & Rorden, C. Global versus local processing: seeing the left side of the forest and the right side of the trees. *Front. Hum. Neurosci.* **6**, 28 (2012).
76. Delis, D. C., Robertson, L. C. & Efron, R. Hemispheric specialization of memory for visual hierarchical stimuli. *Neuropsychologia* **24**, 205–214 (1986).
77. Robertson, L. C., Lamb, M. R. & Knight, R. T. Effects of lesions of temporal-parietal junction on perceptual and attentional processing in humans. *J. Neurosci.* **8**, 3757–3769 (1988).
78. Robertson, L. C. & Ivry, R. Hemispheric asymmetry: attention to visual and auditory primitives. *Curr. Dir. Psychol. Sci.* **9**, 59–63 (2000).
79. Yovel, G., Levy, J. & Yovel, I. Hemispheric asymmetries for global and local visual perception: effects of stimulus and task factors. *J. Exp. Psychol. Hum. Percept. Perform.* **27**, 1369–1385 (2001).
80. Becker, D. V., Kenrick, D. T., Neuberg, S. L., Blackwell, K. C. & Smith, D. M. The confounded nature of angry men and happy women. *J. Pers. Soc. Psychol.* **92**, 179–190 (2007).
81. Borod, J. C. et al. Right hemisphere emotional perception: evidence across multiple channels. *Neuropsychology* **12**, 446–458 (1998).
82. Silberman, E. K. & Weingartner, H. Hemispheric lateralization of functions related to emotion. *Brain Cogn.* **5**, 322–353 (1986).
83. Tzourio-Mazoyer, N. et al. Automatic anatomical labelling of activations in SPM using a macroscopic anatomical parcellation of the MNI MRI single-subject brain. *Neuroimage* **15**, 273–289 (2002).
84. Denison, R. N., Vu, A. T., Yacoub, E., Feinberg, D. A. & Silver, M. A. Functional mapping of the magnocellular and parvocellular subdivisions of human LGN. *Neuroimage* **102**, 358–369 (2014).
85. Adams, R. B. Jr. et al. Compound facial threat cue perception: contributions of visual pathways, aging, and anxiety. *J. Vis.* **16**, 1375 (2016).
86. Im, H. Y., Adams, R. B., Jr., Boshyan, J., Ward, N., Cushing, C. & Kveraga, K. Anxiety modulates perception of facial fear in a pathway-specific, lateralized manner. Preprint at http://www.biorxiv.org/content/early/2017/05/24/141838 (2017).
87. Kveraga, K. in *Scene Vision: Making Sense of What We See* (eds Kveraga, K. & Bar, M.) 291–307 (MIT Press, Cambridge, MA, 2014).
88. Erk, S., Kleczar, A. & Walter, H. Valence-specific regulation effects in a working memory task with emotional context. *Neuroimage* **37**, 623–632 (2007).
89. Heller, W. & Nitscke, J. B. Regional brain activity in emotion: a framework for understanding cognition in depression. *Cogn. Emot.* **11**, 637–661 (1997).
90. Yang, Q., Wang, X., Yin, S., Zhao, X., Tan, J. & Chen, A. Improved emotional conflict control triggered by the processing priority of negative emotion. *Sci. Rep.* **6**, 24302 (2016).
91. Adams, R. B. Jr. & Kveraga, K. Social vision: functional forecasting and the integration of compound social cues. *Rev. Philos. Psychol.* **6**, 591–610 (2015).
92. Rogers, L. J., Vallortigara, G. & Andrew, R. J. *Divided Brains: The Biology and Behavior of Brain Asymmetries* (Cambridge Univ. Press, Cambridge, 2013).
93. Scott, W. A. Cognitive complexity and cognitive flexibility. *Sociometry* **25**, 405–414 (1962).
94. Craig, A. D. Forebrain emotional asymmetry: a neuroanatomical basis? *Trends Cogn. Sci.* **9**, 566–571 (2005).
95. Davidson, R. J. in *Brain Asymmetry, Cerebral Asymmetry, Emotion, and Affective Style* (eds Davidson, R. J. & Hugdahl, K.) 361–387 (MIT Press, Cambridge, MA, 1995).
96. Ivry, R. B. & Robertson, L. C. *The Two Sides of Perception* (MIT Press, Cambridge, MA, 1998).
97. Carroll, N. C. & Young, A. W. Priming of emotion recognition. *Q. J. Exp. Psychol.* **58**, 1173–1197 (2005).
98. Norman, D. A. & Shallice, T. in *Consciousness and Self-Regulation: Advances in Research and Theory IV* (eds Davidson, R., Schwartz, R. & Shapiro, D.) 376–390 (Plenum Press, New York, NY, 1986).
99. Posner, M. I., Rueda, M. R. & Kanske, P. in *Handbook of Psychophysiology* (eds Cacioppo, J. T., Tassinary, J. G. & Berntson, G. G.) 410–414 (Cambridge Univ. Press, Cambridge, 2007).
100. Cant, J. S., Sun, S. Z. & Xu, Y. Distinct cognitive mechanisms involved in the processing of single objects and object ensembles. *J. Vis.* **15**, 1–21 (2015).
101. Chong, S. C., Joo, S. J., Emmmanouil, T. & Treisman, A. Statistical processing: not so implausible after all. *Percept. Psychophys.* **70**, 1327–1334 (2008).
102. Chong, S. C. & Evans, K. K. Distributed vs. focused attention (count vs. estimate). *Wiley Interdiscip. Rev. Cogn. Sci.* **2**, 634–638 (2011).
103. Chong, S. C. & Treisman, A. Attentional spread in the statistical processing of visual displays. *Percept. Psychophys.* **67**, 1–13 (2005).
104. Haberman, J., Brady, T. F. & Alvarez, G. A. Individual differences in ensemble perception reveal multiple, independent levels of ensemble representation. *J. Exp. Psychol. Gen.* **144**, 432–446 (2015).
105. Myczek, K. & Simons, D. J. Better than average: alternatives to statistical summary representations for rapid judgments of average size. *Percept. Psychophys.* **70**, 772–788 (2008).
106. Cant, J. S. & Xu, Y. The impact of density and ratio on object-ensemble representation in human anterior-medial ventral visual cortex. *Cereb. Cortex* **25**, 4226–4239 (2015).
107. Cant, J. S. & Xu, Y. The contribution of object shape and surface properties to object-ensemble representation in anterior-medial ventral visual cortex. *J. Cogn. Neurosci.* **29**, 398–412 (2017).
108. Huis In 't Veld, E. M. J. & de Gelder, B. From individual fear to mass panic. The neurological basis of crowd perception. *Hum. Brain Mapp.* **36**, 2338–1351 (2015).
109. Utochkin, I. S. Ensemble summary statistics as a basis for rapid visual categorization. *J. Vis.* **15**, 1–14 (2015).
110. Brady, T. F. & Alvarez, G. A. No evidence for a fixed object limit in working memory: ensemble representations inflate estimates of working memory capacity for complex objects. *J. Exp. Psychol. Learn. Mem. Cogn.* **41**, 921–929 (2015).
111. Cohen, M. A., Dennett, D. C. & Kanwisher, N. What is the bandwidth of perceptual experience? *Trends Cogn. Sci.* **19**, 324–335 (2016).
112. Feigenson, L. in *Space, Time, and Number in the Brain: Searching for the Foundations of Mathematical Thought* (eds Dehaene, S. & Brannon, E.) 13–22 (Elsevier, London, 2011).
113. Im, H. Y. & Chong, S. C. Mean size as a unit of visual working memory. *Perception* **43**, 663–676 (2014).

© 2017 Macmillan Publishers Limited, part of Springer Nature. All rights reserved.

114. Im, H. Y., Park, W. J. & Chong, S. C. Ensemble statistics as units of selection. *J. Cogn. Psychol.* **27**, 114–127 (2015).
115. Cowan, N. The magical number 4 in short-term memory: a reconsideration of mental storage capacity. *Behav. Brain Sci.* **24**, 87–185 (2001).
116. Luck, S. & Vogel, E. K. The capacity of visual working memory for features and conjunctions. *Nature* **390**, 279–281 (1997).
117. Pylyshyn, Z. W. & Storm, R. W. Tracking multiple independent targets: evidence for a parallel tracking mechanism. *Spat. Vis.* **3**, 179–197 (1988).
118. Treisman, A. M. & Gelade, G. A feature-integration theory of attention. *Cogn. Psychol.* **12**, 97–136 (1980).
119. Haberman, J. & Whitney, D. in *From Perception to Consciousness: Searching with Anne Treisman* (eds Wolfe, J. & Robertson, L.) Ch. 16 (Oxford Univ. Press, Oxford, 2012).
120. Brady, T. F. & Alvarez, G. A. Hierarchical encoding in visual working memory: ensemble statistics bias memory for individual items. *Psychol. Sci.* **22**, 384–392 (2011).
121. Cohen, J. *Statistical Power Analysis for the Behavioral Sciences* (Lawrence Erlbaum Associates, Hillsdale, NJ, 1988).
122. Brainard, D. H. The Psychophysics Toolbox. *Spat. Vis.* **10**, 433–436 (1997).
123. Pelli, D. G. The VideoToolbox software for visual psychophysics: transforming numbers into movies. *Spat. Vis.* **10**, 437–442 (1997).
124. Maule, J. & Franklin, A. Effects of ensemble complexity and perceptual similarity on rapid averaging of hue. *J. Vis.* **15**, 1–18 (2015).
125. Utochkin, I. S. & Tiurina, N. A. Parallel averaging of size is possible but range-limited: a reply to Marchant, Simons, and De Fockert. *Acta Psychologica* **146**, 7–18 (2014).
126. Fitts, P. M. & Seeger, C. M. S-R compatibility: spatial characteristics of stimulus and response codes. *J. Exp. Psychol.* **46**, 199–201 (1953).
127. Deichmann, R., Gottfried, J. A., Hutton, C. & Turner, R. Optimized EPI for fMRI studies of the orbitofrontal cortex. *Neuroimage* **19**, 430–441 (2003).
128. Wall, M. B., Walker, R. & Smith, A. T. Functional imaging of the human superior colliculus: an optimised approach. *Neuroimage* **47**, 1620–1627 (2009).
129. Kringelbach, M. L. & Rolls, E. T. The functional neuroanatomy of the human orbitofrontal cortex: evidence from neuroimaging and neuropsychology. *Prog. Neurobiol.* **72**, 341–372 (2004).
130. Mazaika P. K., Hoeft, F., Glover G. H. & Reiss A. L. Methods and software for fMRI analysis for clinical subjects. In *Poster Session Presented at the Meeting of Human Brain Mapping 2009* (2009).
131. Fischl, B. et al. Automatically parcellating the human cerebral cortex. *Cereb. Cortex* **14**, 11–22 (2004).
132. Spiridon, M., Fischl, B. & Kanwisher, N. Location and spatial profile of category-specific regions in human extrastriate cortex. *Hum. Brain Mapp.* **27**, 77–89 (2006).

Acknowledgements

This work was supported by the National Institutes of Health (R01MH101194) to K.K. and R.B.A. Jr. Data collection was conducted at the Pennsylvania State University. Informed written consent was obtained for all the studies according to the procedures of the Institutional Review Board at the Pennsylvania State University. The participants received a course credit for their participation. No funders had any role in study design, data collection and analysis, decision to publish or preparation of the manuscript.

Author contributions

H.Y.I., R.B.A. Jr and K.K. developed the study concept and all authors contributed to the study design. Testing and data collection were performed by H.Y.I, C.A.C., T.G.S. and D.N.A. H.Y.I analysed the data and all authors wrote the paper.

Competing interests

The authors declare no competing interests.

Additional information

Supplementary information is available for this paper at https://doi.org/10.1038/s41562-017-0225-z.

Reprints and permissions information is available at www.nature.com/reprints.

Correspondence and requests for materials should be addressed to K.K.

Publisher's note: Springer Nature remains neutral with regard to jurisdictional claims in published maps and institutional affiliations.

© 2017 Macmillan Publishers Limited, part of Springer Nature. All rights reserved.

nature research

Corresponding author(s): Kestutis Kveraga

☐ Initial submission ☐ Revised version ☒ Final submission

Life Sciences Reporting Summary

Nature Research wishes to improve the reproducibility of the work that we publish. This form is intended for publication with all accepted life science papers and provides structure for consistency and transparency in reporting. Every life science submission will use this form; some list items might not apply to an individual manuscript, but all fields must be completed for clarity.

For further information on the points included in this form, see Reporting Life Sciences Research. For further information on Nature Research policies, including our data availability policy, see Authors & Referees and the Editorial Policy Checklist.

Experimental design

1. Sample size

Describe how sample size was determined.

Sample size was initially determined based on pilot studies using the same experimental design. A power analysis (N*) based on the pilot run of this experiment with four subjects indicated that 21 subjects were enough to achieve at least 80% power.

2. Data exclusions

Describe any data exclusions.

No subjects were excluded from the behavioral data analysis.
For fMRI study, two participants were excluded from further analyses because they made too many late responses (e.g., RTs longer than 2.5s).

3. Replication

Describe whether the experimental findings were reliably reproduced.

We provided details on all the replicated findings in the supplementary results.

4. Randomization

Describe how samples/organisms/participants were allocated into experimental groups.

We used within-subject design. Because within-subject design was used, no group allocation was needed. The sequence of experimental trials was randomized for each individual subject.

5. Blinding

Describe whether the investigators were blinded to group allocation during data collection and/or analysis.

Investigators were blinded to the randomization of the experimental sequence until the data collection was finished.

Note: all studies involving animals and/or human research participants must disclose whether blinding and randomization were used.

6. Statistical parameters

For all figures and tables that use statistical methods, confirm that the following items are present in relevant figure legends (or in the Methods section if additional space is needed).

n/a	Confirmed
☐	☒ The exact sample size (*n*) for each experimental group/condition, given as a discrete number and unit of measurement (animals, litters, cultures, etc.)
☐	☒ A description of how samples were collected, noting whether measurements were taken from distinct samples or whether the same sample was measured repeatedly
☐	☒ A statement indicating how many times each experiment was replicated
☐	☒ The statistical test(s) used and whether they are one- or two-sided (note: only common tests should be described solely by name; more complex techniques should be described in the Methods section)
☐	☒ A description of any assumptions or corrections, such as an adjustment for multiple comparisons
☐	☒ The test results (e.g. *P* values) given as exact values whenever possible and with confidence intervals noted
☐	☒ A clear description of statistics including central tendency (e.g. median, mean) and variation (e.g. standard deviation, interquartile range)
☐	☒ Clearly defined error bars

See the web collection on statistics for biologists for further resources and guidance.

Software

Policy information about availability of computer code

7. Software

Describe the software used to analyze the data in this study.	FreeSurfer, MATLAB, SPM8, rfxplot, ArtRepair

For manuscripts utilizing custom algorithms or software that are central to the paper but not yet described in the published literature, software must be made available to editors and reviewers upon request. We strongly encourage code deposition in a community repository (e.g. GitHub). *Nature Methods* guidance for providing algorithms and software for publication provides further information on this topic.

Materials and reagents

Policy information about availability of materials

8. Materials availability

Indicate whether there are restrictions on availability of unique materials or if these materials are only available for distribution by a for-profit company.	No unique materials were used.

9. Antibodies

Describe the antibodies used and how they were validated for use in the system under study (i.e. assay and species).	No antibodies were used.

10. Eukaryotic cell lines

a. State the source of each eukaryotic cell line used.	No eukaryotic cell lines were used.
b. Describe the method of cell line authentication used.	No eukaryotic cell lines were used.
c. Report whether the cell lines were tested for mycoplasma contamination.	No eukaryotic cell lines were used.
d. If any of the cell lines used are listed in the database of commonly misidentified cell lines maintained by ICLAC, provide a scientific rationale for their use.	No commonly misidentified cell lines were used.

Animals and human research participants

Policy information about studies involving animals; when reporting animal research, follow the ARRIVE guidelines

11. Description of research animals

Provide details on animals and/or animal-derived materials used in the study.	No animals were used in this study.

Policy information about studies involving human research participants

12. Description of human research participants

Describe the covariate-relevant population characteristics of the human research participants.	A total of 74 subjects (41 female and 33 male) participated in Experiments 1A, 1B, and 2. All of them were undergraduate students in the USA.

nature research

Corresponding author(s): Kestutis Kveraga

☐ Initial submission ☐ Revised version ☒ Final submission

MRI Studies Reporting Summary

Form fields will expand as needed. Please do not leave fields blank.

Experimental design

1. Describe the experimental design.	Event-related design
2. Specify the number of blocks, trials or experimental units per session and/or subject, and specify the length of each trial or block (if trials are blocked) and interval between trials.	Number of trials in each run: 156 trials. Length of each trial: 2.5 seconds Number of runs per subject: 4 runs The total number of the trials per subject: 624 trials.
3. Describe how behavioral performance was measured.	Participants' button press was recorded during the fMRI session. The accuracy (percent of correct button press) and the response time were used for the analyses of the behavioral data during the fMRI experiment. We also used the mean accuracy for each experimental condition and for each participant. Repeated measures ANOVA, post hoc Tukey's HSD pairwise comparison tests, and further contrast analyses using specific weights, and paired t-test analyses were conducted on the accuracy data. For the response time (RT), we primarily used the mean RT and conducted same types of statistical tests, but also verified some of the main results by looking at the median RT.

Acquisition

4. Imaging	
a. Specify the type(s) of imaging.	Functional and anatomical
b. Specify the field strength (in Tesla).	3T
c. Provide the essential sequence imaging parameters.	High resolution anatomical MRI data were acquired using T1-weighted images for the reconstruction of each subject's cortical surface (TR = 2300 ms, TE = 2.28 ms, flip angle = 8˚, FoV = 256 x 256 mm, slice thickness = 1 mm, sagittal orientation). The functional scans were acquired using gradient-echo EPI with a TR of 2000 ms, TE of 28ms, FoV of 240 x 240 mm, flip angle of 52˚ and 64 interleaved slices (3 x 3 x 2 mm, slice thickness = 2 mm).
d. For diffusion MRI, provide full details of imaging parameters.	N/A
5. State area of acquisition.	A whole brain scan was used.

Preprocessing

6. Describe the software used for preprocessing.	The acquired fMRI images were pre-processed using SPM8 (Wellcome Department of Cognitive Neurology) run on MATLAB software.

7. Normalization

a. If data were normalized/standardized, describe the approach(es).

Functional and anatomical images were normalized into standard space using the Montreal Neurological Institute (MNI)-152 template. The SPM software used the normalization procedure to minimize the differences between an image and a MNI template space using a linear, affine transformations (3 translations, 3 rotations, 3 zooms, and 3 shears), then a nonlinear transformations (deformation fields).

b. Describe the template used for normalization/ transformation.

MNI152

8. Describe your procedure for artifact and structured noise removal.

To remove residual variance caused by head movements during the image acquisition, the movement parameters extracted in the realignment procedure were included as additional covariates. During fitting of the data, the time series were filtered with a high-pass filter of 128 s to remove artifacts due to cardio respiratory and other cyclical influences, and corrected for serial correlations.

9. Define your software and/or method and criteria for volume censoring, and state the extent of such censoring.

Outliers due to head movement or signal from preprocessed files, using thresholds of 3 SD from the mean, 0.75 mm for translation and 0.02 radians rotation, were removed from the data sets, using the ArtRepair software (Mazaika et al., 2009).

Statistical modeling & inference

10. Define your model type and settings.

Subject-specific contrasts were estimated using a fixed-effects model. These contrast images were used to obtain subject-specific estimates for each effect.

11. Specify the precise effect tested.

The subject-specific estimates were entered for group analysis into a second-level analysis treating participants as a random effect, using one-sample t-tests at each voxel.

12. Analysis

a. Specify whether analysis is whole brain or ROI-based.

Both whole brain and ROI analyses were used.

b. If ROI-based, describe how anatomical locations were determined.

We defined a separate contrast between all the visual stimulation trials (all trials containing stimuli) vs. background (Null trials). From this contrast, we localized each of the ROIs based on the peak activation within the anatomical label obtained by the anatomical parcellation of the normalized brain (Tzourio-Mazoyer et al., 2002).

13. State the statistic type for inference. (See Eklund et al. 2016.)

The resulting t-test contrasts were thresholded applying a family-wise error (FWE) correction with $p < 0.05$.

14. Describe the type of correction and how it is obtained for multiple comparisons.

FWE was used.

15. Connectivity

a. For functional and/or effective connectivity, report the measures of dependence used and the model details.

N/A

b. For graph analysis, report the dependent variable and functional connectivity measure.

N/A

16. For multivariate modeling and predictive analysis, specify independent variables, features extraction and dimension reduction, model, training and evaluation metrics.

N/A